



How to weigh a fossil mammal? South American notoungulates as a case study for estimating body mass in extinct clades

Allison Nelson¹ · Russell K. Engelman² · Darin A. Croft³

Accepted: 31 May 2023 / Published online: 12 July 2023

© The Author(s), under exclusive licence to Springer Science+Business Media, LLC, part of Springer Nature 2023

Abstract

Body mass (BM) is a fundamental variable for many paleobiological investigations that is challenging to accurately infer for species that lack living representatives and/or close morphological analogs. This study explores this issue using notoungulates, a diverse group of extinct South American herbivorous mammals with an extensive fossil record. We use a new dataset of 1,900+ extant mammal species (from ~80,000 specimens) to estimate notoungulate BM based on head-body length and a published dataset of 400+ species (~2,100 specimens) to estimate BM based on occipital condyle width. Condylabasal length, stylopod diameter and circumference, and neck length data are used to explore factors that can confound BM predictions. We estimate the following BM ranges for 10 osteologically well-characterized species and calculate similar ranges for 30 others known from less complete remains: Toxodontia: *Thomashuxleya externa* (80–120 kg), *Homalodotherium cunninghami* (250–350 kg), *Scarrittia canquelensis* (450–550 kg), *Adinotherium ovinum* (75–90 kg), *Nesodon imbricatus* (350–400 kg), and *Toxodon platensis* 1,000–1,200 kg; Typotheria: *Interatherium robustum* (1.9–2.0 kg), *Miocochilius anomopodus* (9–14 kg), *Prottypotherium australe* (3.5–4.0 kg), and *Pachyrukhos moyani* (1.2–1.6 kg). We suggest that species such as these can be used as “calibration points” when inferring BM of species known from more limited remains. Discrepancies between our estimates and previously-published studies are primarily due to the distinctive craniodental morphology of notoungulates and the robust limb bones of toxodontians. There is significant, non-random error correlated with body habitus (i.e., being relatively robust or gracile) in many variables traditionally used to estimate BM, including femur circumference, and new methods are needed to compensate for this.

Keywords Body mass · Head-body length · Neogene · Occipital condyle width · Notoungulata · SANU

Introduction

Notoungulata are an extinct clade of terrestrial herbivorous mammals that inhabited South America from the early Paleocene through the Late Pleistocene, an evolutionary history

spanning more than 60 million years. From the middle Eocene through the middle Miocene, notoungulates were cornerstones of Neotropical mammal communities and continued to be conspicuous members of terrestrial herbivore guilds until their demise during the late Quaternary extinctions (Patterson and Pascual 1968; Simpson 1980; Marshall et al. 1983; Marshall and Cifelli 1990; Pascual et al. 1996; Croft 2016; Croft et al. 2020). Many notoungulates are known from complete or nearly complete skeletons (e.g., Sinclair 1909; Scott 1912; Riggs 1937; Simpson 1945; Chaffee 1952; Stirton 1953; Shockley 1997; Cerdeño et al. 2012), and many others are known from well-preserved skulls and/or postcrania (e.g., Simpson 1948, 1967; Bocchino de Ringuelet 1957; Villarroel 1974a; Cerdeño and Contreras 2000; Hitz et al. 2000; Croft et al. 2003; Shockley and Anaya 2008; Billet et al. 2009; Shockley et al. 2012; Vera 2012; Guérin and Faure 2013; Giannini and García-López 2014; Fernández-Monescillo et al. 2022). The abundance of notoungulate remains has made it possible for researchers to study many aspects of their paleobiology, particularly within the past decade, which has provided new insights into their

✉ Allison Nelson
nelsonallisone@gmail.com

Russell K. Engelman
neovenatoridae@gmail.com

Darin A. Croft
dcroft@case.edu

¹ Department of Earth and Atmospheric Sciences, Indiana University, 1001 E 10th St., Bloomington, IN 47405, USA

² Department of Biology, Case Western Reserve University, 10900 Euclid Ave., Cleveland, OH 44106, USA

³ Department of Anatomy, Case Western Reserve University School of Medicine, 10900 Euclid Ave., Cleveland, OH 44106-4930, USA

habits and habitats (e.g., Cassini and Vizcaíno 2012; Cassini et al. 2012a, b, 2017; Gomes Rodrigues et al. 2017; Fernández-Monescillo et al. 2018; Sosa and García-López 2018; Ercoli et al. 2019, 2021a, b; Lorente et al. 2019; Croft and Lorente 2021). Nevertheless, because there are no extant notoungulates, correlations between anatomy and ecology are difficult; in some cases, different analyses have reached in disparate or even contradictory conclusions about their paleobiology. This is most clearly apparent in dietary studies (e.g., Croft and Weinstein 2008; Croft et al. 2008; Townsend and Croft 2008; Billet et al. 2009; Cassini et al. 2011, 2012a; Palazzi and Barreda 2012; Strömberg et al. 2013; Dunn et al. 2015; Seoane et al. 2017; Ercoli et al. 2021a), but it also extends to investigations of body size (e.g., Cassini et al. 2012a, b; Croft 2016; Fernández-Monescillo et al. 2019; Croft et al. 2020).

Body size, generally measured as mass, is arguably the single most significant ecological attribute of any organism, as it strongly correlates with numerous biological variables such as diet, population density, home range, basal metabolic rate, locomotor habits, dispersal ability, reproductive behavior, and extinction risk (Bartholomew 1981; Schmidt-Nielsen 1984; Eisenberg 1990; Price and Hopkins 2015). Thus, accurate estimates of body mass are necessary for confidently reconstructing the paleobiology of extinct mammals and the paleoecology of ancient mammal communities. Although estimating the body mass of an extinct mammal always involves uncertainty, these uncertainties are greater for some groups than others. In the case of notoungulates, three main factors have hampered generating reliable estimates: (1) lack of extant representatives; (2) lack of close modern analogs; and (3) the diversity of body plans within the group.

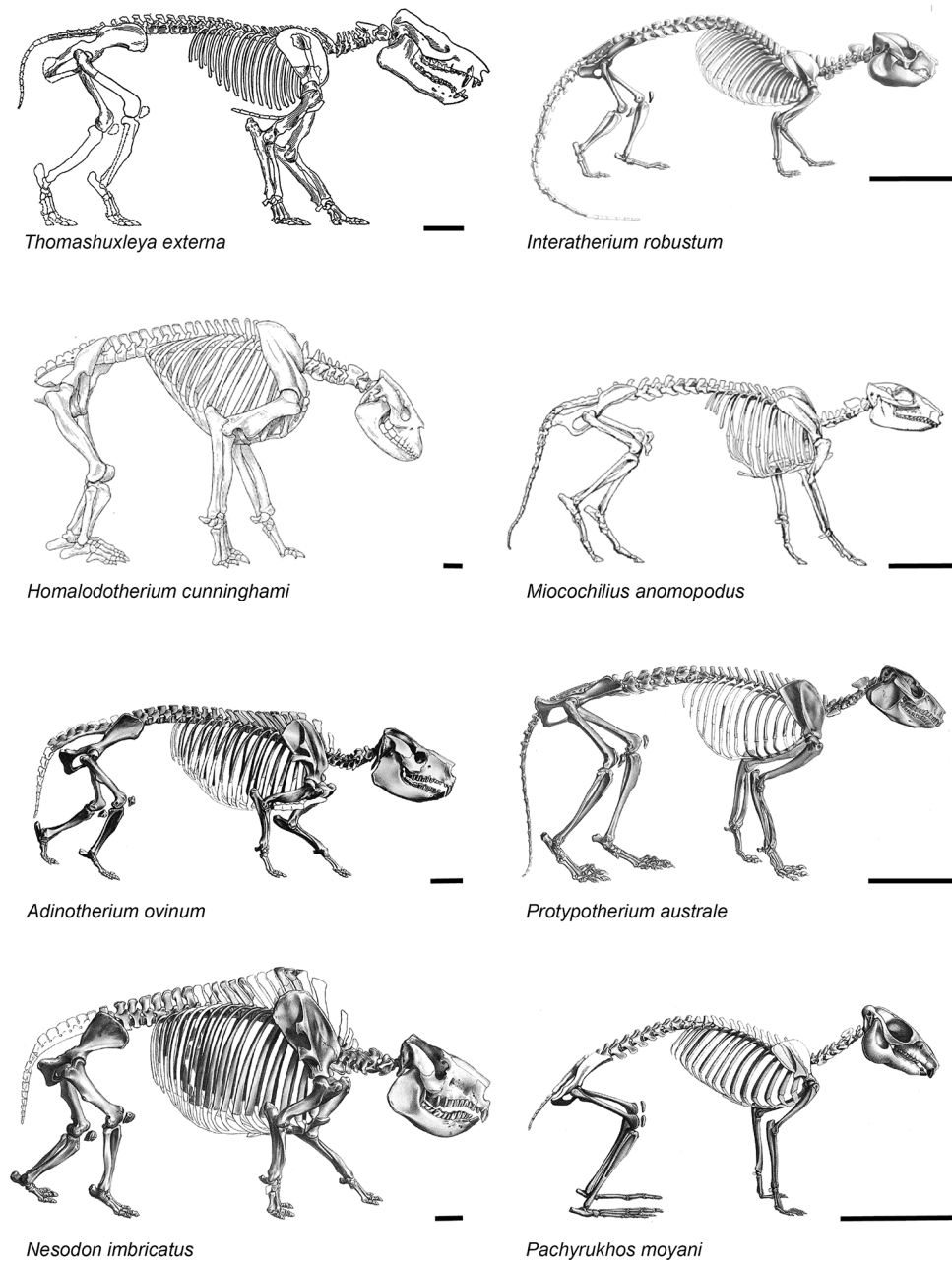
The lack of extant notoungulates makes it impossible to test how different osteological proxies correlate with body mass in this clade, as can be done with most extant mammal groups. As a result, it is not clear which dental, cranial, and/or postcranial variables are most likely to provide the most accurate estimates. One approach to dealing with this problem is to use the average of multiple body mass estimates calculated using different proxies in order to generate a central tendency (e.g., Fariña et al. 1998; Rinderknecht and Blanco 2008; Elissamburu 2012), though the mathematical and theoretical basis for this practice have been questioned (Mendoza et al. 2006; Hopkins 2018). Another approach is to use a very broad range of extant mammals as a comparative dataset to avoid strong correlations that are specific to certain groups; this approach has been used in quantitative studies of locomotor preference in notoungulates (e.g., Shockley et al. 2007; Croft and Anderson 2008) but has yet to be used for notoungulate body mass estimates (though one of the equations used by Elissamburu 2012 was based on a relatively broad dataset). However, unless the anatomical proxy correlates extremely closely with body mass, these

estimates will be very imprecise and/or inaccurate due to the great deal of anatomical variation among mammals. These and other issues were recently reviewed in greater detail by Engelmann (2022).

The lack of extant notoungulates would be less problematic if close anatomical analogs to notoungulates existed today. Although such analogs may exist for certain subgroups (e.g., modern wombats for mesotheriids; Shockley et al. 2007; Sosa and García-López 2018), this is not the case for most notoungulates. Notoungulates differ greatly from extant artiodactyls and perissodactyls – the most diverse groups of modern ungulates and the taxa to which notoungulates are most frequently compared – in both cranial and postcranial features. For example, most Neogene notoungulates have hypselodont postcanine teeth (Patterson and Pascual 1968; Croft 1999; Madden 2015; Gomes Rodrigues et al. 2017; Croft et al. 2020). To accommodate such high-crowned teeth, the proportions of notoungulate skulls differ from those of most extant ungulates, complicating efforts to use skull shape and certain skull dimensions to infer body mass. Similarly, occlusal dimensions of very hypsodont and hypselodont teeth can change as they develop and undergo wear (Madden 1990; Kramarz 2002; Croft et al. 2003), and this attribute must be taken into consideration when using dental proxies to estimate body mass. Postcranially, most notoungulates have few cursorial adaptations (Croft and Lorente 2021) or are graviportal, unlike most extant ungulates, which could be problematic for body mass proxies based on limb proportions. Although many notoungulates resemble rodents or rabbits in certain aspects of their anatomy (Sinclair 1908; Seckel and Janis 2008; Ercoli et al. 2019), they are not closely similar overall. The chimeric anatomy of notoungulates is highlighted by the title of Owen's (1838: p. 16) description of the first known member of the group, the rhino-sized Late Pleistocene *Toxodon platensis*: "A gigantic extinct mammiferous animal, referable to the Order Pachydermata, but with affinities to the Rodentia, Edentata, and Herbivorous Cetacea."

In addition to the unusual combination of features present in all notoungulates, there is considerable variation within the group in terms of overall size and proportions (Fig. 1). For example, Pliocene *Paedotherium typicum* (a pachyrukhine similar to *Pachyrukhos moyani*; Fig. 1, lower right) tended toward cursoriality (Elissamburu 2004; Elissamburu and Vizcaíno 2005), inhabited burrows (Cardonatto and Melchor 2018), and was about the size of a mara (Dolichotinae). By contrast, Pleistocene *Toxodon platensis* (similar to *Nesodon imbricatus*; Fig. 1, lower left) was a large-headed, graviportal megamammal (Bond 1999; MacFadden 2005). Even within this great range of body size diversity, there was also significant ecomorphological diversity, including: long-necked members of Leontiniidae (e.g., *Scarritia canquensis* and *Taubatherium paulacoutoi*; Chaffee 1952; Couto-Ribeiro 2015); fossorial, wombat-like mesotheriids (Shockley et al.

Fig. 1 Skeletal reconstructions of notoungulates, with toxodontians in the left column and typotheres in the right. Head-body length and image sources as follows: *Adinotherium ovinum*, 136 cm, from Scott (1912: pl. XII); *Homalodotherium cunninghami*, 189 cm, from Riggs (1937: fig. 55); *Nesodon imbricatus*, 213 cm, from Scott (1912: pl. XII); *Thomashuxleya externa*, 134 cm, from Simpson (1967: fig. 35); *Interatherium robustum*, 41 cm, from Sinclair (1909: pl. IX); *Miocochilius anomopodus*, 73 cm, from Stirton (1953: pl. 8); *Pachyrukhos moyani*, 33 cm, from Sinclair (1909: pl. XI); *Protypotherium australe*, 57 cm, from Sinclair (1909: pl. VII). Scale bars equal 10 cm



2007; Fernández-Monescillo et al. 2018); the elongate, ferret-like *Interatherium* spp. (Sinclair 1909; Fig. 1, upper right); and the plantigrade, clawed, chalicotheriid-like *Homalodotherium cunninghami* (Riggs 1937; Elissamburu 2010; Fig. 1, left column). Other notoungulates show more generalized body plans, such as Eocene *Thomashuxleya externa* (Carrillo and Asher 2017; Fig. 1, upper left) and late Oligocene *Eurygenium pacegnum* (Shockley 1997: fig. 5). Four to six families of notoungulates are recorded at most middle Cenozoic sites in South America (Croft 2016), a diversity that could have been supported only through substantial ecological (and morphological) diversity among species.

The primary goal of our study is to generate new body mass estimates for notoungulates using variables that correlate strongly with body mass in terrestrial mammals that have not yet been applied extensively to notoungulates: head-body length (Damuth 1990; Prothero 1992; Silva and Downing 1995) and occipital condyle width (Engelman 2022). We use an original, extensive modern comparative dataset of head-body length data compiled from more than 1,900 species and nearly 80,000 specimens to create new predictive equations for generating body mass estimates using species mean values. Predictive equations for occipital condyle width are based on the dataset of Engelman

(2022). Body mass estimates based on other variables (including condylobasal length and femur circumference) are used to explore factors that can potentially confound body mass estimates in extinct taxa, such as body habitus. We compare our new notoungulate body mass estimates to previously published estimates and analyze potential explanations for discrepancies.

Materials and methods

Comparative dataset

As a starting point for this analysis, we obtained head-body length (HBL; total length minus tail length) and body mass (BM) data from digitized museum catalogs in VertNet (vertnet.org), ARCTOS (arctos.database.museum), the Smithsonian Museum of Natural History (<https://collections.nmnh.si.edu/search/mammals/>), the American Museum of Natural History (<https://emu-prod.amnh.org/db/emuwebamnh/index.php>), the Sam Noble Museum of Natural History, the Australian Museum, and AQUILA of the Naturmuseum Senckenberg (<https://search.senckenberg.de/aquila-public-search/search>). These two measurements are ones that most mammalogists systematically record when collecting voucher specimens (Ansell 1956; Naughton 2012) and are often included in digital collections. Because these data come from field tag data in museum collections, it is not possible to control for interobserver error. However, since HBL has a standard definition and method of measurement (Ansell 1956; Naughton 2012) this error is likely to be limited. When compiling the dataset, a greater effort was made to include larger-bodied taxa (e.g., artiodactyls, perissodactyls, carnivorans) than smaller-bodied ones (e.g., shrews, murid rodents) because our study focuses on extinct mammals with $BM > 1 \text{ kg}$. These data were subsequently augmented with data from the published literature as well as data collected by the authors from other non-digitized museum collections (see Online Resource 1).

The composite dataset was double-checked record-by-record in order to eliminate clear outliers, ensure consistency in data collection, and omit individuals that did not appear to be mature adults. Individuals were deemed unreliable based on information recorded on the specimen voucher (e.g., specimens explicitly identified as immature or gravid at time of capture), comparisons with the broader sample (e.g., a specimen $< 75\%$ the size of any other specimen of the same species), or a dramatically large or small BM (suggesting a possible lapsus, such as a value recorded in imperial units rather than metric). Although we do not have precise data for the number of individuals excluded, we estimate that roughly 1% of specimens were excluded due to potentially unreliable data. This resulted in a refined dataset

of 70,412 observations. These data were then augmented with data from 159 additional studies in which mean HBL and BM values (rather than individual values) were reported for an entire sample, but HBL and BM were measured in all specimens (Online Resource 1). These two datasets were combined by multiplying sample means from these pooled studies by the number of specimens in the sample and then averaging all observations for that species in the dataset (in effect, retaking the mean of the entire sample). This resulted in a dataset of 1,907 species derived from 79,968 individuals. It is important to note that all HBL and BM values were collected from the same samples (i.e., the same individuals), averting potential statistical issues with drawing these data from different samples. A complete list of specimens, institutions, and references used to collect the data can be found in Online Resource 1.

Occipital condyle width data were taken from Engelmann (2022), in which occipital condyle width (OCW) and BM were collected from a dataset of 2,127 specimens representing 404 mammal species (Online Resource 2). Occipital condyle width was measured as the greatest bilateral width across the occipital condyles, and BM was estimated using the model that included the categorical conditions of “monotreme-like” and “rabbit-like” condyles as additional variables (see Engelmann 2022: p. 13–14). All notoungulates were considered to lack these specialized states. Some pachyrhynchine notoungulates have occipital condyles that are slightly narrower than expected (Ercoli et al. 2021b: fig. 5), but the condition in these taxa is closer to the ancestral state for mammals than the derived state present in lagomorphs. In this dataset, as in the HBL and BM dataset described above, all OCW and BM data are paired (i.e., they derive from the same individuals). However, samples of OCW and HBL in the present study generally were not collected from the same individuals because the data were taken from independent studies.

Neck length, body habitus, and condylobasal length

When estimating BM based on HBL, it is assumed that a mammal’s body approximates a cylinder and that variations from this generally cylindrical form are relatively minor (Damuth 1990; Prothero 1992). Two attributes that could violate this assumption and create errors in correlation are neck length (NL) and body habitus. If the neck of a mammal is significantly longer or shorter than that of the average of the sample, the length of its body cylinder (and therefore its BM) will be overestimated or underestimated, respectively. Similarly, if a mammal’s body habitus (i.e., its mass or thickness relative to the length of its body or limbs) is significantly more robust or gracile than that of an average mammal, the diameter of its body cylinder (and therefore its BM), will be underestimated or overestimated, respectively.

Both of these potentially confounding variables are relevant to questions of body mass estimation in South American native ungulates (including notoungulates). South American native ungulates generally seem to have more robust limb bones than most extant ungulates (Croft and Anderson 2008; Carrillo and Asher 2017; McGrath et al. 2018), and several families are characterized by elongate necks (e.g., macrauheniid litopterns and leontiniid notoungulates; Scott 1910; Chaffee 1952).

To examine the effects of neck length (NL) and body habitus on mass estimates, we collected NL data (calculated as the summed vertebral body lengths of C1–7) and stylopod (femur and humerus) midshaft measurements for 313 species in this study using data from the published literature (Online Resource 1). Due to the limited availability of data, these measurements were not available for every taxon and could not be drawn from the same individuals for which HBL and BM were measured. However, since mammals exhibit determinate growth, differences among individuals should be small enough to permit testing the potential effects of body habitus on BM estimates.

Percent neck length (%NL) was calculated by dividing NL by the mean HBL for the species. Body habitus was examined using four midshaft stylopod measurements: humerus mediolateral diameter, humerus circumference, femur mediolateral diameter, and femur circumference. For each species, four “robustness indices” were calculated by dividing each stylopod measurement by mean HBL. These indices quantify limb bone thickness relative to body size independent of BM, making them suitable for testing the relationship between body habitus and BM. We analyzed all four measurements to explore potential differences in quantifying body habitus, but since they all produced similar results (see Online Resource 3: Section 11), we focus our discussion on the femur circumference (FC) robustness index (RI); this had the largest sample size among the robustness indices we analyzed and is generally thought to correlate well with BM (e.g., Anderson et al. 1985; Roth 1990; Ruff 1990; Anyonge 1993; Christiansen 1999; Sánchez-Villagra et al. 2003; Campione and Evans 2012).

Craniodontal measurements are correlated with BM in extant ungulates and have been used to estimate BM in extinct artiodactyls and perissodactyls (e.g., Mendoza et al. 2006) as well as notoungulates (e.g., Cassini et al. 2012b). Nevertheless, notoungulates may have had relatively large heads for their body size (Sinclair 1908; Simpson 1945; Carrillo and Asher 2017; Croft et al. 2020), which could result in overestimates of BM based on such measurements. We added condylobasal length (CbL) to our comparative dataset to test the hypothesis that CbL results in greater mass estimates for notoungulates than HBL and other variables. Condyllobasal length is generally considered equivalent

to skull length in studies of mammals and is preferred over greatest length of the skull since the latter is often measured oblique to the anteroposterior axis and may include the overhanging nasals or nuchal crest. By contrast, CbL is much easier to compare across taxa. Body mass estimates based on CbL were calculated using the equation of Engelman (2022), which used literature data on condylobasal length and body mass data from voucher tags (not from the same individuals) in a sample of 404 species (see Online Resource 2).

Data analysis

All analyses were performed in R 4.1.1 (R Core Team 2021) using the packages *ape* (Paradis and Schliep 2018), *broom* (Robinson et al. 2022), *DT* (Xie et al. 2022), *ggfortify* (Horikoshi and Tang 2016), *gridExtra* (Auguie 2017), *kableExtra* (Zhu 2021), *nlme* (Pinheiro et al. 2019), *nlstools* (Baty et al. 2015), *readxl* (Wickham and Bryan 2022), *scales* (Wickham and Seidel 2022), *stringr* (Wickham 2022), and *tidyverse* (Wickham et al. 2019). Results can be found in Online Resource 3, which includes a link to download the original R code (.rmd format) at the top of the document.

We used an ordinary least squares (OLS) model in this study rather than a phylogenetic generalized least squares (PGLS) model for two main reasons. First, we ran both models, and support statistics such as Akaike information criterion (AIC) and Bayesian information criterion (BIC) were better for the OLS model than for the PGLS model. Second, using PGLS for data that span all of Mammalia is problematic due to the way current PGLS R packages calculate the best-fit line (see Engelman 2022 for details). Specifically, PGLS models are constructed using two sources of data: measurement data and phylogenetic information (branch lengths). Both are necessary to accurately predict values for new taxa under a PGLS model. For example, if an unknown taxon is a member of Felidae, it would be expected to show a similar deviation relative to the best-fit line (residual) as other felids. Indeed, this observation of non-independent residuals was the original impetus for developing phylogenetic comparative methods like PGLS (see Symonds and Blomberg 2014). However, the resulting best-fit line produced by a PGLS model predicts values for new taxa without considering the effect of phylogeny on the resulting estimation, treating it as an OLS line. The actual slope and intercept of a PGLS allometric model vary depending on the phylogenetic position of the taxon being considered. By contrast, the singular reported best-fit line in most R packages is statistically equivalent to the allometric relationship for taxa located at the most recent common ancestor of the entire tree (Ane 2021). This occurs even if phylogenetic information is available for the new taxon being considered (e.g., if Notoungulata is added to a phylogeny of extant mammals as

sister to Perissodactyla based on Buckley 2015 and Welker et al. 2015). Thus, PGLS reconstructs phylogeny-free allometric relationships well, but existing PGLS packages tend to predict the values of individual data points poorly.

The issue discussed above is of particular concern for Mammalia; due to the deep divergence between Monotremata and Theria, PGLS places unknown taxa at the most recent common ancestor of these two groups. Because of the extremely divergent morphology of these clades (e.g., sprawling versus erect limbs), Monotremata and Theria often show separate regression lines; thus, an intermediate model fails to accurately describe members of either clade (Engelman 2022). When phylogenetic information is not used to estimate values for new taxa, PGLS models generally perform worse than OLS models in terms of accuracy, likely due to phylogenetic non-independence; like the data used to create the models, data for new taxa are not independent but non-randomly distributed across a phylogeny (Symonds and Blomberg 2014). Theoretical methods for incorporating phylogenetic signal when estimating values for new taxa have been proposed in the literature (Garland and Ives 2000), but none of the major PGLS packages in R currently include this functionality.

Fossil taxa and data collection

We analyzed 40 species of notoungulates (Table 1). For 17 of these species, full skeletons or skeletal reconstructions were available that allowed HBL to be measured in addition to OCW and/or CbL. For the remaining 23 notoungulate species, only OCW and/or CbL data were available. Measurements were collected from the published literature or measured firsthand from specimens or casts. We did not exclude any skeletal reconstructions a priori. However, as detailed in the Discussion, it became apparent through our analyses that one published reconstruction (the notohippid *Eurygenium pacegnum*) is likely inaccurate. Measurements, sources, and other data are provided in Appendix (see also Online Resource 4).

Measurements of HBL from published articulated skeletal reconstructions were made using ImageJ (Schneider et al. 2012). We measured HBL along the curves of the reconstructed spinal column from the anterior tip of the rostrum to the posterior end of the sacrum while providing some allowance for soft tissue of the neck *in vivo* between the nuchal process of the skull and the dorsal processes of the anterior thoracic vertebrae (Fig. 2). Since the nuchal ligament in most mammals extends directly between the dorsalmost point of the nuchal crest and the neural spines of the anterior thoracic vertebrae, the amount of missing soft tissue in the neck can be approximated relatively easily in a skeleton. The measurement for HBL used for fossil specimens here is equivalent

to measuring HBL “over curves”, the primary method of measuring HBL in studies of extant mammals (Ansoll 1956; Naughton 2012). In a prone mammal, this value is typically measured along the dorsal curves of the spine; in a supine mammal, it is typically measured along a straight line, from the tip of the rostrum to the posterior end of the sacrum. In both cases, HBL is measured from the tip of the snout to the sacro-caudal joint. Occipital condyle width was measured as the greatest bilateral width across the occipital condyles, following Engelman (2022). Condyllobasal length was measured as the length from the anterior tip of the premaxillae to the posterior end of the occipital condyles (Elbroch 2006). Femur circumference data were taken from Carrillo and Asher (2017) and Elissamburu (2012). In all cases, notoungulate BM was estimated using the complete corresponding extant dataset described above. Additionally, when possible, notoungulate BM was calculated using a factor to correct for body habitus (an issue discussed further below).

For eight of the notoungulates we analyzed, more than 20 body mass estimates have been published using different approaches. We used Google Sheets to generate histograms of these estimates on a \log_{10} scale to facilitate comparisons between these estimates and the new ones generated here (see Discussion: Notoungulate body mass estimates).

Several notoungulate families probably do not represent natural (monophyletic) groups, at least as traditionally conceived (Cifelli 1993; Shockley 1997; Croft et al. 2003; Billet et al. 2009; Cerdeño and Vera 2010; Reguero and Prevosti 2010; Billet 2011; Shockley et al. 2012; Perini et al. 2022). Nevertheless, due the paleoecological focus of our study, we use these names without quotation marks to avoid unnecessarily encumbering the results and discussion.

Anatomical and analytical abbreviations BM: body mass; CbL: condyllobasal length (= skull length); FC: femur circumference; HBL: head-body length; NL: neck length; OCW: occipital condyle width; PE: prediction error; PE_{cf}: prediction error with correction factor; RI: robustness index; SEE: standard error of the estimate.

Institutional abbreviations AC: Beneski Museum of Natural History, Amherst, U.S.A.; AMNH: American Museum of Natural History, New York, USA; FC-DPV: Colección de Vertebrados Fósiles: Facultad de Ciencias, Montevideo, Uruguay; FMNH PM: Fossil Mammal Collection, The Field Museum, Chicago, USA; FUMDHAM: Fundação do Museu do Homem Americano, São Raimundo Nonato, Brazil; IGM: Museo Geológico Nacional, Servicio Geológico Colombiano (formerly INGEOMINAS), Bogotá, Colombia; MACN-A: Ameghino Collection, Museo Argentino de Ciencias Naturales “Bernardino Rivadavia”, Buenos Aires, Argentina; MACN-Pv:

Table 1 Age and provenance data for notoungulate species analyzed in this study

Species	Family (Suborder)	Locality	Country (Province)	Geologic Unit	Age	Occurrence Reference(s)
<i>Adinotherium ovinum</i>	Toxodontidae (Tx)	Santa Cruz	Argentina (Santa Cruz)	Santa Cruz Formation	Early Miocene (Burdigalian)	Scott (1912)
<i>Archaeohyrax patagonicus</i>	Archaeohyracidae* (Ty)	Cabeza Blanca	Argentina (Chubut)	Upper Puesto Almendra Member (Sarmiento Formation)	Late Oligocene (Chattian)	Billet et al. (2009)
<i>Archaeotylotherium tinguitiricense</i>	Archaeohyracidae* (Ty)	Tinguitirica	Chile (Bernardo O'Higgins)	Abanico Formation	Early Oligocene (Rupeilian)	Croft et al. (2003)
<i>Charratoxodon uruguayensis</i>	Toxodontidae (Tx)	Arazáff	Uruguay (San José)	Raión Formation	Late Pliocene – Early Pleistocene	Ferrero et al. (2022)
<i>Chasicotherium rothi</i>	Homalodotheriidae (Tx)	Arroyo Chasicó	Argentina (Buenos Aires)	Arroyo Chasicó Formation	Late Miocene (Tortonian)	Cabrera and Kraglievich (1931)
<i>Eurygenium pacenum Gualla cayana</i>	Notohippidae* (Tx)	Salla	Bolivia (La Paz)	Salla Beds	Late Oligocene (Chattian)	Shockley (1997)
	Leontiniidae (Tx)	Quebrada Fiera	Argentina (Mendoza)	Agua de la Piedra Formation	Late Oligocene (Chattian)	Cerdeño and Vera (2015)
<i>Hegetotherium mirabile</i>	Hegetotheriidae (Ty)	Puesto Estancia La Costa	Argentina (Santa Cruz)	Santa Cruz Formation	Early Miocene (Burdigalian)	Sinclair (1909)
<i>Hemihegetotherium trilobus</i>	Hegetotheriidae (Ty)	Quebrada Honda	Bolivia (Tarija)	Honda Group	Middle Miocene (Serrvallian)	Croft and Anaya (2006)
<i>Homalodotherium cuninghami</i>	Homalodotheriidae (Tx)	Santa Cruz	Argentina (Santa Cruz)	Santa Cruz Formation	Early Miocene (Burdigalian)	Scott (1930)
<i>Huiatherium pluriplicatum</i>	Leontiniidae (Tx)	La Venta	Colombia (Huila)	Honda Group	Middle Miocene (Serrvallian)	Villarroel and Colwell Danis (1997)
<i>Interatherium robustum</i>	Interatheriidae (Ty)	Santa Cruz	Argentina (Santa Cruz)	Santa Cruz Formation	Early Miocene (Burdigalian)	Sinclair (1909)
<i>Leontinia gaudryi</i>	Leontiniidae (Tx)	Cabeza Blanca	Argentina (Chubut)	Upper Puesto Almendra Member (Sarmiento Formation)	Late Oligocene (Chattian)	Loomis (1914)
<i>Mendozhippus fierensis</i>	Notohippidae* (Tx)	Quebrada Fiera	Argentina (Mendoza)	Agua de la Piedra Formation	Late Oligocene (Chattian)	Cerdeño and Vera (2010)
<i>Mesotherium cristatum</i>	Mesotheriidae (Ty)	Toscas del Río de La Plata	Argentina (Buenos Aires)	Ensenada Formation	Late Pliocene – Early Pleistocene	Tonni et al. (1999)
<i>Microtylotherium choquecatense</i>	Mesotheriidae (Ty)	Choquecota	Bolivia (Oruro)	Choquecota Formation	Middle Miocene (Langhian)	Villarroel (1974b)
<i>Miocochilus anomopodus</i>	Interatheriidae (Ty)	La Venta	Colombia (Huila)	Honda Group	Middle Miocene (Serrvallian)	Stirtton (1953)
<i>Nesodon imbricatus</i>	Toxodontidae (Tx)	Santa Cruz	Argentina (Santa Cruz)	Santa Cruz Formation	Early Miocene (Burdigalian)	Scott (1912)
<i>Nesodon taveretus</i>	Toxodontidae (Tx)	San Rafael Dept	Argentina (Mendoza)	Aisol Formation (lower section)	Early Miocene (Burdigalian)	Forasiepi et al. (2015)

Table 1 (continued)

Species	Family (Suborder)	Locality	Country (Province)	Geologic Unit	Age	Occurrence Reference(s)
<i>Notopithecus adarinus</i>	Interatheriidae (Ty)	Gran Barranca	Argentina (Chubut)	Gran Barranca Member (Sarmiento Formation)	Middle Eocene (Bartonian)	Vera (2016)
<i>Notostylops murinus</i>	Notostylopidae	Gran Barranca	Argentina (Chubut)	Gran Barranca Member (Sarmiento Formation)	Middle Eocene (Bartonian)	Simpson (1948)
<i>Pachyrhukhos moyani</i>	Hegetotheriidae (Ty)	Santa Cruz	Argentina (Santa Cruz)	Santa Cruz Formation	Early Miocene (Burdigalian)	Sinclair (1909)
<i>Paedotherium bonaerense</i>	Hegetotheriidae (Ty)	(Uncertain)	Argentina (Buenos Aires)	(Uncertain)	Pliocene to early Pleistocene (Zanclean to Gelasianiacenian)	Cerdeño and Bond (1998)
<i>Paedotherium typicum</i>	Hegetotheriidae (Ty)	Tio Punco and Barranca de Los Lobos	Argentina (Tucumán and Buenos Aires)	Andalhuala and Chapadmal formations (not listed)	Pliocene (Zanclean and Piacenzian)	Armella (2019); MacPhee (2014)
<i>Piauhytherium capivarae</i>	Toxodontidae (Tx)	Lagoa dos Porcos	Brazil (Piauí)		Late Pleistocene	Guérin and Faure (2013)
<i>Plesiotypotherium achi-</i> <i>rense</i>	Mesotheriidae (Ty)	Achiri	Bolivia (Potosí)		Late Miocene (Tortonian)	Villarroel (1974a)
<i>Plesiotypotherium cas-</i> <i>rense</i>	Mesotheriidae (Ty)	Casira	Bolivia (Potosí)	Casira Formation	Late Miocene?	Cerdeño et al. (2012)
<i>Proudinothereum muen-</i> <i>steri</i>	Toxodontidae (Tx)	Gran Barranca	Argentina (Chubut)	Colhue-Huapi Member (Sarmiento Formation)	Early Miocene (Aquitian–Burdigalian)	Madden (1990)
<i>Prosotherium garzoni</i>	Hegetotheriidae (Ty)	Scarritt Pocket	Argentina (Chubut)	Upper Puesto Almendra Member (Sarmiento Formation)	Late Oligocene (Chatitian)	Chaffee (1952)
<i>Protypotherium australe</i>	Interatheriidae (Ty)	Santa Cruz	Argentina (Santa Cruz)	Santa Cruz Formation	Early Miocene (Burdigalian)	Sinclair (1909)
<i>Protypotherium prae-</i> <i>titulum</i>	Interatheriidae (Ty)	Santa Cruz	Argentina (Santa Cruz)	Santa Cruz Formation	Early Miocene (Burdigalian)	Sinclair (1909)
<i>Pseudotypotherium</i> <i>pulchrum</i>	Mesotheriidae (Ty)	Farola Monte Hermoso	Argentina (Buenos Aires)	Monte Hermoso Formation	Pliocene (Zanclean)	Fernández-Monescillo et al. (2022)
<i>Pseudotypotherium</i> <i>subinsigne</i>	Mesotheriidae (Ty)	Huayquerias de San Carlos	Argentina (Mendoza)	Tunuyán Formation	Pliocene (Zanclean)	Cerdeño (2019)
<i>Rhynchippus equinus</i>	Notohippidiae* (Tx)	Scarritt Pocket	Argentina (Chubut)	Upper Puesto Almendra Member (Sarmiento Formation)	Late Oligocene (Chatitian)	Chaffee (1952)
<i>Scarritia canquensis</i>	Leontiniidae (Tx)	Scarritt Pocket	Argentina (Chubut)	Upper Puesto Almendra Member (Sarmiento Formation)	Late Oligocene (Chatitian)	Chaffee (1952)
<i>Taubatherium paulo-</i> <i>couoi</i>	Leontiniidae (Tx)	Tremembé	Brazil (Sao Paulo)	Tremembé Formation	Late Oligocene (Chatitian)	Soria and Alvarenga (1989)
<i>Thomashuxleya extrema</i>	Isotomidae* (Tx)	Cañadón Vaca	Argentina (Chubut)	Sarmiento Formation	Middle Eocene (Lutetian)	Carrillo and Asher (2017)
<i>Toxodon platensis</i>	Toxodontidae (Tx)	(Various)	Argentina (Buenos Aires)	Pampean Formation	Late Pleistocene	Fariña et al. (1998)

Table 1 (continued)

Species	Family (Suborder)	Locality	Country (Province)	Geologic Unit	Age	Occurrence Reference(s)
<i>Tremacyllus impressus</i>	Hegetotheriidae (Ty)	Farola Monte Hermoso	Argentina (Buenos Aires)	Monte Hermoso Formation	Early Pliocene (Zanclean)	Cerdeño and Bond (1998)
<i>Typhotheriopsis chasicensis</i>	Mesotheriidae (Ty)	Arroyo Chasicó	Argentina (Buenos Aires)	Arroyo Chasicó Formation	Late Miocene (Tortonian)	Croft et al. (2004)

Species are listed in alphabetical order. Families that are likely non-monophyletic are indicated by an asterisk (*), and suborder is indicated by Tx (Toxodontia) and Ty (Typotheria)

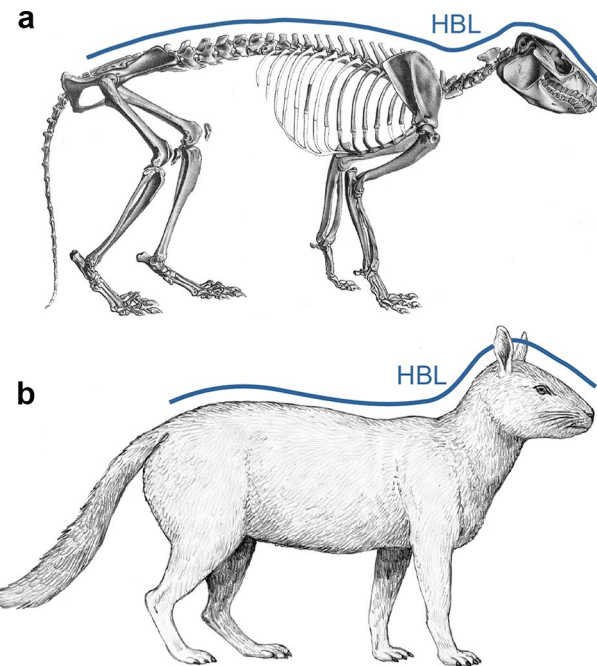
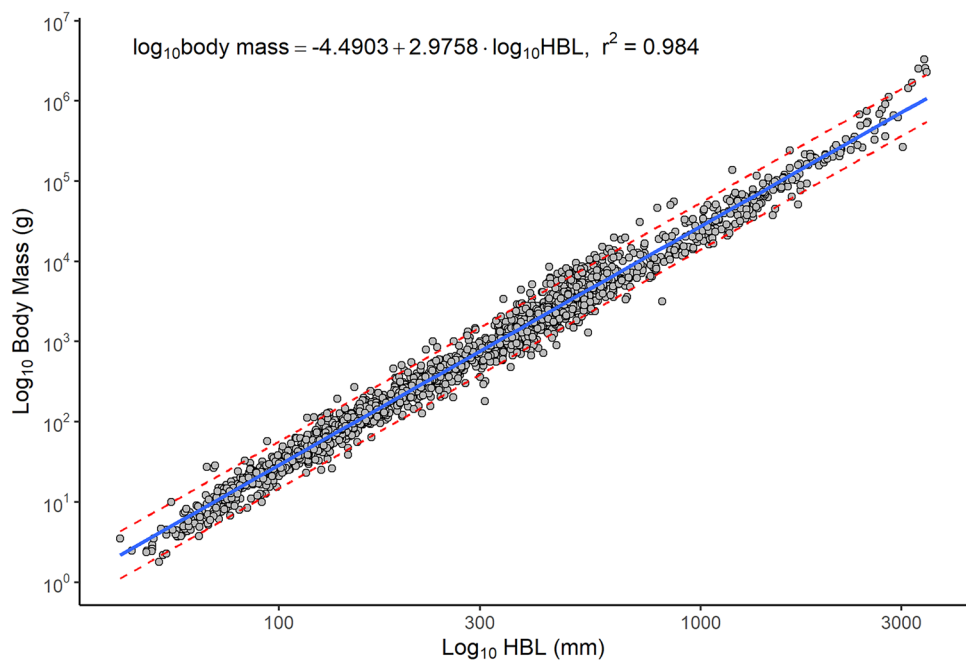


Fig. 2 Illustration of how head-body length (HBL) was measured in this study, using the interatheriid notoungulate *Protypotherium australe* as an example. The method is based on how HBL is typically measured in extant mammals: from the tip of the snout (or skull) to the base of the tail (or distal end of the sacrum), following curves. **a.** skeletal reconstruction (from Sinclair 1909: pl. IX); **b.** life reconstruction (from Cassini et al. 2012a: fig. 14.3a)

vertebrate paleontology collection, Museo Argentino de Ciencias Naturales “Bernardino Rivadavia”, Buenos Aires, Argentina; MCNAM-PV: Vertebrate Paleontology Collection, Museo de Ciencias Naturales y Antropológicas “J. C. Moyano”, Mendoza, Argentina; MHN: Museu de Historia Natural e Jardim Botânica, Pontifícia Universidade Católica de Minas Gerais, Brazil; MHNSR-PV: Museo de Historia Natural de San Rafael, San Rafael, Argentina; MHNT-VPPLT: Museo de Historia Natural la Tatacoa, Villavieja, Colombia; MLP: Museo de La Plata, La Plata, Argentina; MMP: Museo Municipal de Ciencias Naturales de Mar del Plata, Mar del Plata, Argentina; MNHN: Muséum national d’Histoire naturelle, Paris, France; MNHN-BOL-V: Vertebrate Paleontology Collection, Museo Nacional de Historia Natural, La Paz, Bolivia; MHNT-VPPLT: Museo de Historia Natural La Tatacoa, Villavieja, Colombia; PVL: Paleontología Vertebrados Lillo, Tucumán, Argentina; SGOPV: vertebrate paleontology collections, Museo Nacional de Historia Natural, Santiago, Chile; UCMP: University of California Museum of Paleontology, Berkeley, California, USA; USNM: Smithsonian National Museum of Natural History, Washington D.C., USA; YPM VPPU: Princeton University Collection, Yale Peabody Museum, New Haven, USA.

Fig. 3 Scatterplot of body mass vs. head-body length (on a log₁₀ scale) for all extant species in this study



Results

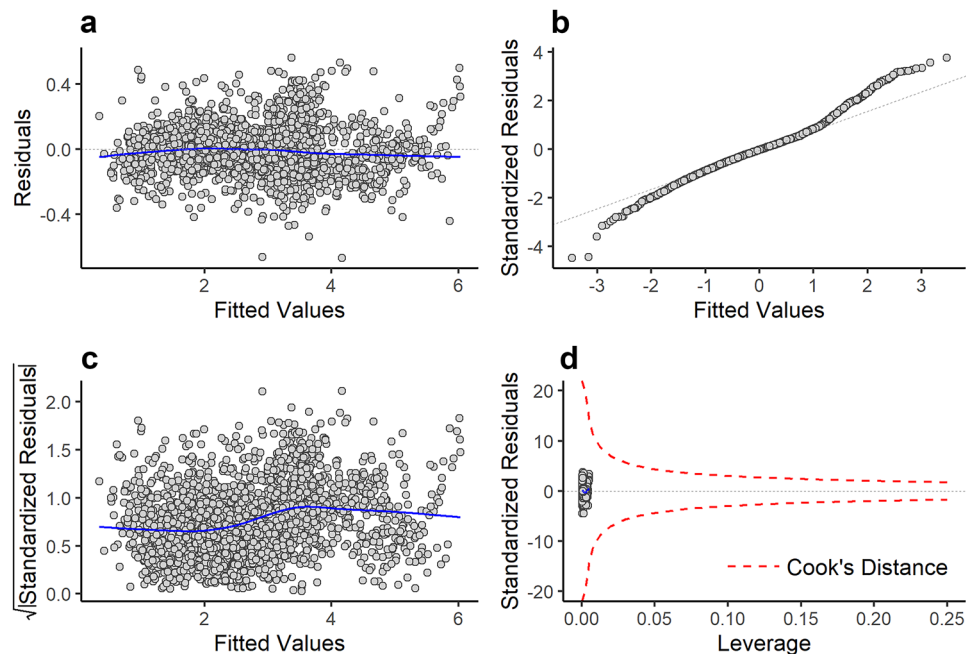
Head-body length

In extant mammals, log-transformed HBL and BM strongly correlate with one another (Fig. 3), with a correlation coefficient (r^2) of 0.9837. The regression model has an overall percent prediction error with correction factor (%PE_{cf}) of $\pm 26.41\%$. This error rate makes the model highly accurate result by the standards of mammalian body

mass regression equations, where error rates < 33% are rare (Van Valkenburgh 1990; Ruff 2003; Engelman 2022).

Diagnostic plots of the model suggest the resulting best-fit model is appropriate for linear regression. The residuals versus fits plot (Fig. 4a) suggests the residuals are randomly distributed and suggest a linear relationship between the log-transformed variables. The residuals of the model are normally distributed in a Q-Q plot (Fig. 4b), though with a slight tail in the upper quantile. The scale-location plot (Fig. 4c) shows a slight increase in heteroskedasticity at

Fig. 4 Diagnostic plots of the all-species regression equation. **a.** residuals versus fitted values plot; **b.** Q-Q plot **c.** scale-location plot; **d.** residual versus leverage



3 kg, but this appears to be driven by the high residuals among primates (discussed further below) rather than overall model heteroskedasticity. Running the model excluding primates removes this spike in residuals (see Online Resource 3: Section 4.2.1). Finally, the residuals versus leverage plot (Fig. 4d) indicates that no single data point or set of data points has disproportionate influence on the best-fit line.

Testing for a non-linear fit of the data under a power rule produces a log-allometric exponent of 0.923 (95% confidence interval = 0.859–0.987). This suggests the overall distribution of the data approximates log-linearity. The fact that the log-allometric exponent does not overlap with 1 may be due to systematically large, positive residuals in graviportal ungulates making the best fit loess line slightly non-linear, though this does not appear to be strictly a result of size (see Discussion). When transformed back to an arithmetic scale and written as a power law, HBL and BM scale to a relationship of $HBL \propto BM^{0.2976}$. This is close to the theoretical expectation of geometric similarity between a linear and volumetric measurement ($HBL \propto BM^{0.33}$).

One potential concern for reconstructing BM in extinct species > 1 kg such as notoungulates is that including many extant mammals smaller than this in the model might produce inaccurate estimates. Restricting the comparative dataset to taxa > 1 kg results in a best-fit line that is nearly identical to that produced when all species are included (Online Resource 3: Section 9, Fig. 9.1). The regression line based on all taxa > 1 kg has a slight upward trend at lower BM compared to the all-species regression model. However, this is due to the large number of primates and cingulates at the lower end of this range (1–10 kg). Primates and cingulates show high errors in the all-species regression model, and because a large proportion of mammals in the 1–10 kg range are primates this results in the regression line only considering mammals > 1 kg to be pulled upward. By contrast, considering all mammals and including smaller mammals in the dataset reduces the biasing effects of primates and cingulates. Similarly, when primates and cingulates are excluded from the analysis of taxa > 1 kg, the resulting PE_{cf} is comparable to that for the all-taxon model (27.5% vs. 26.41%, respectively); when they are included, PE_{cf} is greater (33.89%).

When the dataset is arbitrarily separated at a certain size threshold to test whether the allometric relationship between HBL and BM is consistent across the entire dataset, both slope and intercept are found to be significantly different when the data are divided into categories of greater or less than 1 kg (slope: $t = -1.998$, $p = 0.046$; intercept: $t = 3.198$, $p = 0.00142$) and greater or less than 10 kg (slope: $t = -2.625$, $p = 0.009$; intercept: 2.702 , $p = 0.007$). However, this is due to the presence of primates and large, graviportal ungulates like elephantids, rhinocerotids, and hippopotamids at the extremes of the binned

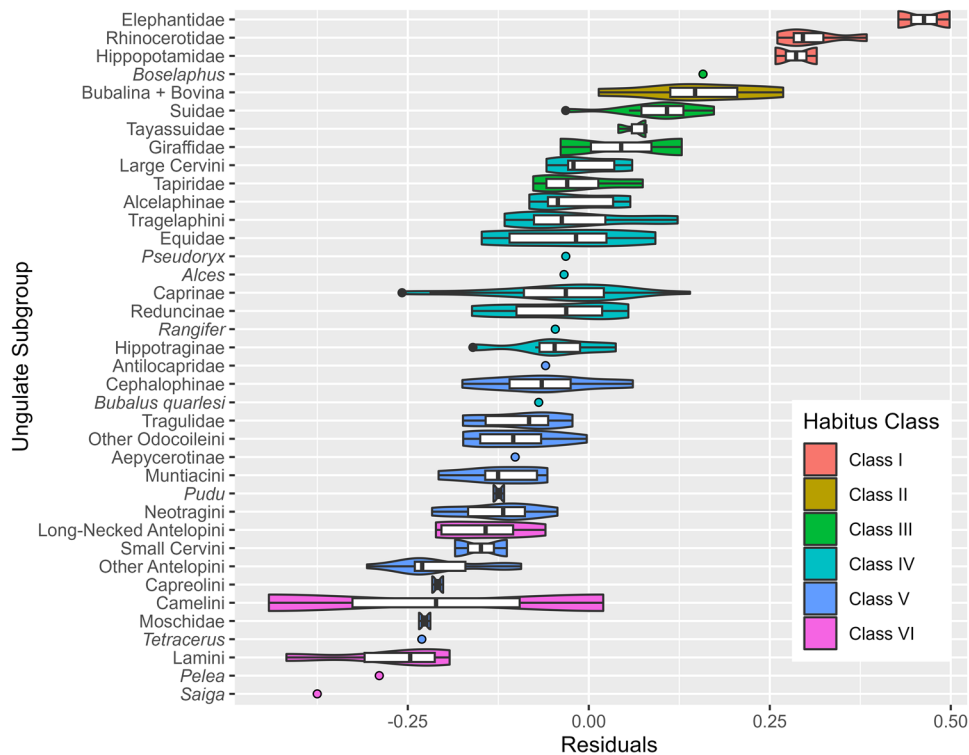
data for the larger size class, which distorts the regression line. Excluding these groups results in slopes and intercepts that do not significantly differ between greater and less than 1 kg bins (slope: $t = -0.492$, $p = 0.623$; intercept: $t = 1.020$, $p = 0.308$) and greater and less than 10 kg bins (slope: $t = -0.001$, $p = 1.000$; intercept: $t = 0.227$, $p = 0.821$) (see Online Resource 3 for additional details).

Body habitus and head-body length

Head-body length does not estimate BM perfectly nor uniformly across mammals. Body mass is underestimated (i.e., there are very high positive residuals) for primates, myrmecophagous mammals (Pholidota, Cingulata, Tubilidentata, and Monotremata), Vombatidae, Erinaceidae, and large, graviportal ungulates (Elephantidae, Rhinocerotidae, and Hippopotamidae). Body mass is underestimated for Mustelidae and other small carnivoran families with a “weasel-like” body plan. Indeed, there appears to be a general correlation between the residual error of the HBL model and the body habitus of a given species. This can be thought of as how massive (or broad) a mammal’s limbs and body are relative to the animal’s overall length.

The effect of body habitus is perhaps best seen in ungulates, in which the residuals of the regression model generally correlate with the general spectrum of graviportality to cursoriality seen in extant ungulates. This allows taxa to be loosely grouped into classes based on their residuals that generally correlate with body habitus (Fig. 5, Table 2). As mentioned above, some of the greatest underestimates of BM (60% or more; Online Resource 3: Table 8.1.1) are in large, graviportal ungulates like elephantids, rhinocerotids, and hippopotamids (Class I in Table 2). Class II includes “typical” bovine bovids such as *Syncerus*, *Bubalus*, and *Bison*, which are heavyset and subcursorial but not graviportal (e.g., still unguigrade; Scott 1985). Class III includes suids, tayassuids, and tapirids, which exhibit a generalized body plan and are typically considered to be non-cursorial. This category also includes giraffids, which are cursorial but have a heavy body habitus due to their very large size. BM is slightly underestimated in Class III mammals. Class IV includes several groups of heavy-set yet cursorial ungulates such as equids, *Alces* (moose), large cervin cervids (i.e., *Cervus elaphus*, *Rusa unicolor*, *Axis* spp.), and alcelaphine, tragelaphine, hippotragine, and caprine bovids. Groups at the more negative end of this interval (i.e., reduncines, cervins, and hippotragines) tend to be comparatively gracile. These taxa have residuals that bracket zero. Class V is composed of smaller-bodied, “classic” cursorial ungulates, such as odocoileins, aepycerotins, antelopins, capreolins, some of the more gracile cervins (e.g., *Dama dama* and *Cervus nippon*) and antilocaprids, as well as the various groups of “slinkers” (sensu Geist 1998): very small, largely forest-dwelling

Fig. 5 Boxplot of residuals in ungulates separated by ungulate subgroup (order, family, subfamily, or tribe) and sorted by mean residuals, showing how residuals of the head-body length (HBL) vs. body mass (BM) regression equation are positively correlated with body habitus (i.e., they increase with more robust postcranial bones). Color-coding in this figure refers to groups defined in Table 2



ungulates that include cephalophines, muntiacins, tragulids, neotragins, moschids, the odocoilein *Pudu*, and *Tetracerus*. In this group, BM is overestimated by 25% or more. Finally, Class VI includes ungulates with an extremely gangly, “hypergracile” build, most with long necks (camelids, *Litocranius*, *Ammodorcas*, and the shorter-necked *Saiga* and *Pelea*). *Nanger*, the other extant long-necked antelopin,

shows lower residuals than *Ammodorcas* and *Litocranius*, but this may be a consequence of its large size among antelopins. These taxa typically have their weight overestimated by 37.5% using HBL. The fact that the residuals of the regression model map onto the generally recognized spectrum of graviportal to cursoriality in ungulates suggests a deeper issue is present.

Table 2 Extant ungulates qualitatively categorized along a spectrum of body habitus and form, from graviportal mammals with short necks (Class I) to highly cursorial mammals with long necks (Class VI)

Group	Examples	N	Residuals	Morphology
Class I	Elephantidae, Hippopotamidae, Rhinocerotidae	9	$\bar{x} = 0.338$ (0.258–0.498)	Graviportal with columnar limbs; very large and heavy-set
Class II	Very large Bovidae (<i>Bison</i> , <i>Bos</i> , <i>Syncerus</i>)	6	$\bar{x} = 0.150$ (0.014–0.268)	Subcursorial and not fully graviportal but heavy-set
Class III	Giraffidae, Suidae, Tapiridae, Tayassuidae, some Bovidae	21	$\bar{x} = 0.070$ (-0.077 to 0.173)	Generalized terrestrial (neither cursorial nor graviportal)
Class IV	Some Bovidae (Alcelaphinae, Caprinae, Reduncini), some Cervidae (<i>Alces</i> , large Cervini), Equidae	63	$\bar{x} = -0.033$ (-0.258 to 0.140)	Cursorial but heavy-set among cursorial ungulates
Class V	V1: Antilocapridae, some Bovidae (Aepycerotinae, Antelopini), some Cervidae (small Cervini, Odocoileini) V2: Moschidae, Tragulidae, some Bovidae (Neotragini, <i>Tetracerus</i>), some Cervidae (<i>Pudu</i>)	66	$\bar{x} = -0.130$ (-0.306 to 0.061)	V1: “Typical” ungulates, cursorial and moderately gracile V2: conspicuously gracile, very small “slinkers”
Class VI	Camelidae, some Bovidae (<i>Saiga</i>)	13	$\bar{x} = -0.224$ (-0.442 to 0.020)	Extremely gracile morphology with elongate necks and limbs

Categories are defined based on external body shape and residuals from the regression of HBL on BM presented in this study. Class I ungulates have the most positive residuals (i.e., BM is underestimated) and Class VI ungulates have the most negative residuals (BM is overestimated). “Slinkers” (sensu Geist 1998) and “typical” ungulates could not be reliably separated using these data even though they seem to represent two different body types within Class V

A similar pattern of correlation between residuals and body habitus is also present among carnivorans. The greatest positive residuals (i.e., actual BM is much greater than expected) are observed in heavyset, fossorial species with well-developed limbs like Taxidiinae and Melinae, followed by the ambulatory and much larger Ursidae. The residuals show a general correlation between increasingly negative values and increasingly gracile postcrania until, at the upper end of the range of variation, the highest negative residuals are observed in several groups of carnivorans with elongate body shapes (and thus, BM much lower than expected based on HBL); these include mustelids, prionodontids, viverrids, and some herpestids (see Online Resource 3: Fig. 7.1). These taxa have the highest overestimates of BM in the entire dataset (often > 50%).

Beyond ungulates and carnivorans, high positive or negative residuals generally correlate with a robust or gracile body habitus, respectively. The taxa noted previously as having high positive residuals (dasypodids, manids, orycteropodids, erinaceids, vombatids and, to a lesser degree, hystricids and *Marmota*) are heavyset, fossorial, and have well-developed limb bones compared to a generalized mammal. Among these, cingulates and pholidotans also bear armor, but since their residuals are no higher than those of armorless mammals of similar habitus (e.g., vombatids and orycteropodids), the weight of armor does not seem to contribute substantially to higher BM residuals. Primates also have high residuals in our analysis, but since they are not particularly robust mammals, this may be due to how HBL was measured in these taxa (see [Discussion](#)).

A regression of the residuals of the all-taxon BM-HBL model against the FC robustness index shows a significant relationship ($t = 16.67$, $p < 0.001$), with a moderate correlation between the two variables ($r^2 = 0.4178$; see Fig. 6a). Functional groups that might be expected to influence this relationship, such as bipedal taxa, monotremes, and primates, do not show a different pattern of correlation (see

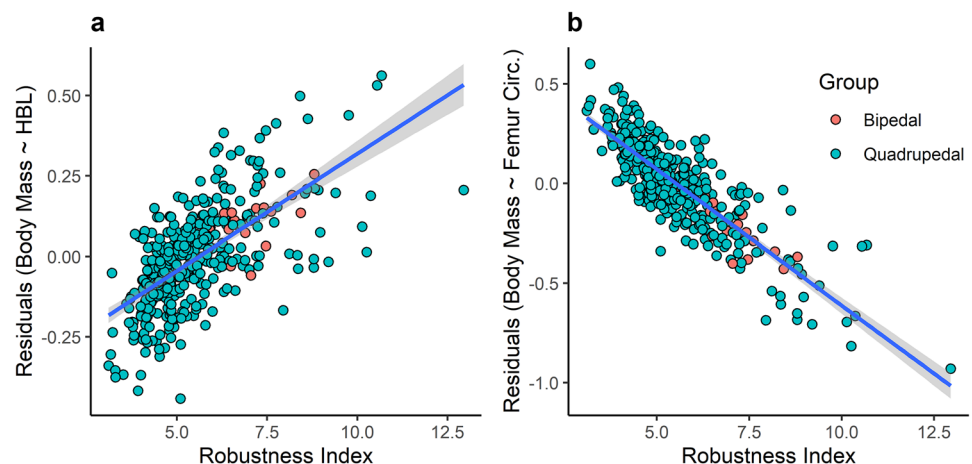
Online Resource 3: Fig. 11.4). Slightly weaker correlations are obtained when the robustness index is calculated using other skeletal measurements, including humerus circumference ($r^2 = 0.3073$, $t = 12.57$, $p < 0.001$), humerus diameter ($r^2 = 0.2973$, $t = 12.63$, $p < 0.001$), and femur diameter ($r^2 = 0.3627$, $t = 13.04$, $p < 0.001$). This combination of high p-values and moderate r^2 values indicates that, while there is not a perfect correlation between the residuals of the BM-HBL model and robustness index (that is, much of the variation is attributable to other factors), body habitus still accounts for a non-negligible proportion of the residual variation seen between BM and HBL. The relatively low r^2 values may be a consequence of HBL and stylopodial dimensions not being drawn from the same individuals.

Neck length

Neck length is strongly correlated with HBL ($r^2 = 0.91$) and shows positive allometry, with larger mammals having proportionately longer necks (allometric exponent = 1.25). This seems to be primarily driven by patterns within Artiodactyla, Perissodactyla, and Carnivora, as excluding these clades greatly reduces the allometric slope (log slope = 1.12). Overall, there is a statistically detectable relationship between %NL and the residuals of the regression equation ($t = -6.838$, $p < 0.001$), but relatively little variation is explained by this relationship ($r^2 = 0.131$). If NL produced a systematic bias it would be expected that taxa with proportionally longer necks (greater %NL) would show progressively greater overestimates of body mass. There is some evidence that an effect is present (Online Resource 3: Section 10.6) but the overall correlation is not strong.

Fitting a multivariate model to HBL and BM considering NL as an additional variable finds NL to have a statistically detectable effect with negative magnitude ($t = -6.29$, $p < 0.001$). Mathematically, this makes intuitive sense; a negative magnitude for the NL coefficient means that relatively

Fig. 6 Graph of the residuals for the regression between head-body length (HBL) and body mass (left) and femur circumference and body mass (right) versus “robustness index” (a mass-free quantification of body habitus)



longer necks need to be downweighted to account for their proportions and produce more accurate BM estimates. The resulting multivariate model has an r^2 of 0.979, %PE_{cf} of 31.41%, and a %SEE of 47.71%. This model results in only a slight improvement in %PE (3%) compared to one that does not take NL into account. Among taxa with very long necks such as giraffids, camelids, *Litocranius walleri*, and *Nanger* spp., models including NL generated more accurate BM estimates in about 2/3 of cases and less accurate BM estimates the others (see Online Resource 3: Table 10.2).

Notoungulate body mass estimates

Notoungulate BM estimates based on HBL are generally larger than those based on OCW for small to medium-sized species (i.e., < 100 kg) and smaller for larger species (Table 3; Appendix). Exceptions to this general pattern include: (1) the small hegetotheriid *Pachyrukhos moyani*, in which HBL BM (1.3 kg) is slightly less than OCW BM (1.6 kg); (2) the small toxodontid *Adinotherium ovinum*, in which HBL BM (77.3 kg) is slightly lower than OCW BM (83.9 kg); and (3) the leontiniid *Taubatherium paulacoutoi*, a large notoungulate in which HBL BM (162.5 kg) is slightly higher than OCW BM (157.6 kg). In several smaller notoungulates, including the interatheriids *Notopithecus adapinus* and *Miocochilius anomopodus* and the hegetotheriid *Paeotherium typicum*, HBL BM is ca. 1.5–2.5 × OCW BM. Large discrepancies between HBL and OCW BM estimates are observed in three large notoungulates; BM based on HBL is close to half that based on OCW for two of these, the homalodotheriid *Homalodotherium cunninghami* and the toxodontid *Nesodon imbricatus*, and it is a mere 1/8th OCW BM for the third species, *Toxodon platensis*, the greatest discrepancy among any pair of variables in our study.

The relationship between HBL and CbL BM estimates in notoungulates resembles that observed for HBL and OCW (i.e., HBL tends to yield larger BM estimates in small to medium species and smaller BM estimates in large species), though differences tend to be smaller (Table 3; Appendix). Exceptions to the overall pattern of greater HBL than CbL BM estimates for notoungulates < 100 kg include: (1) the hegetotheriid *Prosotherium garzoni*, in which HBL BM (2.0 kg) is half CbL BM (4.0 kg); and (2) the notohippid *Eurygenium paceatum*, in which HBL BM (13.4 kg) is only about one-quarter CbL BM (48.4 kg). Among small notoungulates, HBL BM is 1.7 × CbL BM for the hegetotheriid *Paeotherium typicum*; most other CbL BM estimates are within ca. 33% of the corresponding HBL BM estimate. Among large notoungulates, HBL BM of *Toxodon platensis* is only about one-half that based on CbL.

Body mass estimates based on OCW tend to be greater than those based on CbL in medium and large notoungulates (≥ 10 kg) and less than CbL estimates in small notoungulates

(Table 3; Appendix). Exceptions to this pattern include several small typhotheres (*Prototyphotherium praerutilum*, *Pachyrukhos moyani*, and *Interatherium robustum*), in which OCW BM can be ca. 25–50% larger than CbL BM in particular specimens, and several medium to large toxodontians (the isotemnid *Thomashuxleya externa*, the leontiniid *Taubatherium paulacoutoi*, and the notohippid *Rhynchippus equinus*), in which OCW BM is ca. 65–85% that of CbL BM. Outliers among medium and large notoungulates include several toxodontids (*Nesodon imbricatus*, *Nesodon taweretus*, and *Piauhytherium capivarae*), the leontiniid *Leontinia gaudryi*, and the mesotheriid *Typhotheriopsis chasicoensis*; for all of these, OCW estimates for at least some specimens are 1.5–2.25 × those based on CbL. For the toxodontids *Charruatoxodon uruguayensis* and *Toxodon platensis*, OCW BM estimates are nearly triple those based on CbL. Among small notoungulates, outliers include the interatheriids *Notopithecus adapinus* and *Miocochilius anomopodus*, in which OCW BM is about 40–75% that based on CbL.

The observation that BM estimates based on CbL are not consistently greater than those based on HBL or OCW does not support the hypothesis that notoungulates in general had disproportionately long heads.

Discussion

Patterns of variation between head-body length and body mass

We find that HBL predicts BM with a high degree of accuracy across a wide sample of extant mammals representing multiple high-level clades. This supports the idea that mammalian body mass can be mathematically modeled as a cylinder. The applicability of this relationship across almost all of Mammalia suggests it provides a reasonable phylogenetic bracket for inferring BM of extinct therian groups such as Notoungulata. Nevertheless, although this model functions well for most extant mammals (e.g., carnivorans, rodents, most ungulates), it consistently underestimates BM in a few groups, including megafaunal, graviportal ungulates (i.e., “pachyderms” in older parlance) and primates (for which BM is typically underestimated by more than 40%; see Online Resource 3: Table 8.4).

For megamammals, underestimates in BM based on HBL are likely related to body habitus, a topic that is discussed further below. For primates, the discrepancy may be related to methodology. In most mammals, HBL is measured along the dorsal surface of the body, from the tip of the snout to the base of the tail (Ansell 1956; Naughton 2012). By contrast, in primates, HBL is often measured as crown-rump length: from the crown of the head to the base of the tail (see Schultz 1929; Zihlman and Underwood 2013). This

Table 3 Mean body mass (BM) estimates (in kg) for notoungulate species based on condylobasal length (CbL), femoral circumference (FC), head-body length (HBL), and occipital condyle width (OCW)

Species	Family	CbL	FC#	HBL	HBL#	OCW	HBL/CbL	HBL/OCW	OCW/CbL	Estimated Range
<i>Notostylops murinus</i>	Notostylopidae	4.0	-	-	-	2.7	-	-	67.5%	4–10
SUBORDER TOXODONTIA										
<i>Thomashuxleya externa</i> *	Isotemnidae	117.8	114.9	92.2	105.3	73.5	78.3%	125.4%	62.4%	80–120
<i>Chasicotherium rothi</i>	Homalodotheriidae	403.2	-	-	-	360.1	-	-	89.3%	250–350
<i>Homalodotherium cunninghami</i>	Homalodotheriidae	305.0	205.7	202.7	1028.5	360.4	66.5%	56.2%	118.2%	250–350
<i>Gualia cuyana</i>	Leontiniidae	254.2	-	-	-	313.2	-	-	123.2%	250–350
<i>Huiatherium pluriplicatum</i>	Leontiniidae	416.4	-	-	-	465.2	-	-	111.7%	375–500
<i>Leontinia gaudryi</i>	Leontiniidae	265.8	-	-	-	439.0	-	-	165.2%	250–350
<i>Scarrithia canquensis</i> *	Leontiniidae	495.8	333.2	418.4	530.6	-	84.4%	-	-	450–550
<i>Taubatherium paulacoutoi</i>	Leontiniidae	185.1	-	162.5	-	157.6	87.8%	103.1%	85.1%	150–200
<i>Eurygenium paegeum</i>	Notohippididae	48.4	-	13.4	-	-	27.7%	-	-	35–50
<i>Mendozahippus fierensis</i>	Notohippididae	41.7	-	-	-	49.1	-	-	117.7%	35–50
<i>Rhynchoshippus equinus</i>	Notohippididae	46.8	-	-	-	32.0	-	-	68.4%	35–50
<i>Adinotherium ovinum</i> *	Toxodontidae	74.9	92.4	77.3	84.5	83.9	103.2%	92.1%	112.0%	75–90
<i>Charraiaoxodon uruguayensis</i>	Toxodontidae	542.1	-	-	-	1608.6	-	-	296.7%	500–600
<i>Nesodon imbricatus</i> *	Toxodontidae	395.1	390.3	292.0	363.3	624.8	73.9%	46.7%	158.1%	350–400
<i>Nesodon taveretus</i>	Toxodontidae	371.4	-	-	-	597.0	-	-	160.7%	330–380
<i>Piauhytherium capivarae</i> *	Toxodontidae	1107.0	-	-	-	2086.5	-	-	188.5%	700–800
<i>Proadinothereum muensteri</i>	Toxodontidae	141.1	-	-	-	178.1	-	-	126.2%	140–180
<i>Toxodon platensis</i> *	Toxodontidae	1594.1	630.9	728.5	889.7	4404.0	45.7%	16.5%	276.3%	1000–1200
SUBORDER TYPOTHERIA										
<i>Interatherium robustum</i> *	Interatheriidae	1.6	2.0	2.0	1.9	1.9	125.0%	105.3%	118.8%	1.9–2.0
<i>Miocochilus anomopus</i> *	Interatheriidae	9.5	14.3	10.9	13.4	4.7	114.7%	231.9%	49.5%	9–14
<i>Notopithecus adapis</i> *	Interatheriidae	1.1	-	1.3	-	0.5	118.2%	260.0%	45.5%	1.0–1.5
<i>Protypotherium australe</i> *	Interatheriidae	3.7	4.1	3.5	3.7	2.8	94.6%	125.0%	75.7%	3.5–4.0
<i>Protypotherium praeavilium</i>	Interatheriidae	2.4	-	-	-	3.7	-	-	154.2%	2.5–3.0
<i>Mesotherium cristatum</i>	Mesotheriidae	94.0	-	102.4	-	105.5	108.9%	97.1%	112.2%	90–110
<i>Microtypotherium choquecotense</i>	Mesotheriidae	-	-	-	-	13.5	-	-	-	10–15
<i>Plestotypotherium achiense</i> *	Mesotheriidae	29.9	-	40.7	-	32.4	136.1%	125.6%	108.4%	30–40
<i>Plestotypotherium castrense</i>	Mesotheriidae	61.0	-	-	-	75.2	-	-	123.3%	60–75
<i>Pseudotypotherium pulchrum</i>	Mesotheriidae	-	-	-	-	58.0	-	-	-	60–90
<i>Pseudotypotherium subinsigne</i>	Mesotheriidae	-	-	-	-	140.7	-	-	-	90–110
<i>Typotheriopsis chacoensis</i>	Mesotheriidae	49.9	-	-	-	84.9	-	-	170.1%	50–65
<i>Archaeohyracidae</i>	Archaeohyracidae	12.3	-	-	-	9.5	-	-	77.2%	9–13
<i>Archaeoryctotherium tinguiriricaense</i>	Archaeohyracidae	3.5	-	-	-	3.3	-	-	94.3%	3.0–4.0

Table 3 (continued)

Species	Family	CbL	FC#	HBL	HBL#	OCW	HBL/CbL	OCW/CbL	Estimated Range
<i>Hegetotherium mirabile</i>	Hegetotheriidae	4.9	-	-	-	4.9	-	-	4.5–5.5
<i>Hemihelgetotherium trilobus</i>	Hegetotheriidae	9.3	-	-	-	10.4	-	-	11.1–12.8%
<i>Pachyrukhos moyant*</i>	Hegetotheriidae	1.2	1.4	1.3	1.3	1.6	108.3%	81.3%	1.2–1.6
<i>Paedotherium bonaerense</i>	Hegetotheriidae	1.5	-	-	-	1.1	-	-	1.4–2.0
<i>Paedotherium typicum*</i>	Hegetotheriidae	1.4	2.1	2.4	2.1	1.4	171.8%	177.3%	1.6–2.4
<i>Prosotherium garzoni</i>	Hegetotheriidae	4.0	-	2.0	-	-	50.0%	-	2.5–4.0
<i>Tremacyllus impressus</i>	Hegetotheriidae	0.6	-	-	-	0.6	-	-	0.6–1.0

The pound sign (#) denotes estimates adjusted for body habitus (single specimens; see text for details). Ratios among the unadjusted BM estimates are provided as well as the average BM range (Estimated Range) suggested by our analyses (also in kg; see text for discussion). Species are listed alphabetically within each family, with families arranged in phylogenetic order. Species for which the three principal proxies were measured (i.e., HBL, CbL, and OCW) are in bold; those represented by multiple specimens are marked with an asterisk (*). See Appendix for list of each specimen examined, measurements taken, and resulting BM estimates (including 95% prediction interval)

excludes the rostrum and much of the facial skeleton, which results in smaller a HBL value; as a result, is expected to underestimate BM (as is seen in our study). This could also explain why long-snouted primates like papionins (e.g., *Papio* and *Mandrillus*) have some of the highest errors in body mass estimates. However, this would not explain why BM estimates are more accurate for many strepsirrhines (Indriidae, Cheirogaleidae, Lemuridae, Lorisidae) or may even underestimate body mass. Another possibility is that this is driven by the very short neck and/or rostrum of primates (especially anthropoids). Our analyses indicate that primates do not have significantly shorter necks than other mammal groups for which HBL accurately predicts BM, such as rodents, eulipotyphlans, diprotodontian marsupials, and macroscelideans (see Online Resource 3: Fig. 10.2), but we cannot rule out snout length as a confounding factor, as we were unable to measure unskeletonized primate specimens. In any case, it appears that the HBL dataset used here cannot reliably be used to estimate body mass in primates and that more research is needed to understand the underlying methodological and/or morphological factors.

Among mammals as a group, including neck length (NL) as an additional variable does not significantly improve BM estimates based on HBL (Online Resource 3: Section 10). Although including NL can improve BM estimates for some long-necked species, it generates less accurate BM for others (Online Resource 3: Table 10.2). Since there is no clear pattern among the taxa that pertain to each group, this pattern may warrant further investigation to determine whether it could have a methodological or morphological cause. Additionally, NL could be a more important factor to consider when estimating BM estimation in macraucheniid litopterns, which more broadly resemble the long-necked artiodactyls we analyzed than notoungulates do.

The effects of body habitus

There has been persistent debate regarding the best variable or combination of variables for estimating BM in extinct animals (e.g., see these works and references therein: Damuth and MacFadden 1990; Campione and Evans 2012, 2020; Hopkins 2018; Engelmann 2022). This is because not all anatomical variation is related to size. Theoretically, variation in a particular skeletal measurement can be described by two factors: a scalar value that represents absolute size (independent of bone shape), and a shape value primarily influenced by the organism's ecology, evolutionary affinities, and life habits. Limb bone dimensions have generally been considered to be among the best variables for estimating BM because these bones play a direct role in supporting the weight of the animal (Ruff 1990; Campione and Evans 2012). In this context, measurements of weight-supporting limb bone structures, such

as midshaft dimensions (diameter, circumference, cross-sectional area) and areas of articular surfaces, are assumed to be relatively unaffected by other functional demands or phylogenetic factors (Alexander 1980; Anderson et al. 1985; Swartz 1989; Jungers 1990; Ruff 1990; Scott 1990; Anyonge 1993; Egi 2001; Campione and Evans 2012). However, our study suggests that these types of postcranial measurements may not be more reliable than other variables for estimating BM due to the biasing effects of body habitus.

Although HBL is a strong predictor of BM in our analysis, the residuals of the regression model show systematic bias: taxa with a robust body habitus have negative residuals (i.e., BM is underestimated), whereas gracile taxa have positive residuals (i.e., BM is overestimated). Some of the largest errors in BM prediction occur with large, graviportal ungulates of extremely heavy body habitus, such as elephantids, rhinocerotids, and hippopotamids. However, these errors cannot be attributed to allometry in body proportions coupled with very large size, as it also affects smaller members of these groups such as *Choeropsis liberiensis* (the pygmy hippo). This species is relatively small compared to other graviportal ungulates (242 kg vs. > 700 kg) and within the BM range of cursorial ungulates such as equids and large cervids. Nevertheless, residuals and error rates for *C. liberiensis* are comparable to those of *Hippopotamus amphibius* and other graviportal ungulates (PE_{cf} of *C. liberiensis*: -84.3%; PE_{cf} of *H. amphibius*: -61.7). Put another way, *C. liberiensis* has the same body mass as *Equus zebra* or *Cervus elaphus*, even though these other species are 50 cm longer in HBL.

Stylopodial circumferences are generally considered the best proxy for estimating body mass, preferable to both craniodental measurements and axial measurements such as HBL (Alexander 1985; Anderson et al. 1985; Ruff 1990; Campione and Evans 2012; Campione et al. 2014; Campione 2017). However, our data indicate that BM estimates based on limb bone dimensions show the same patterns of bias as those based on HBL. This can be seen in a plot of limb bone robustness (as measured by the FC RI) against the residuals of a regression of log BM on log FC (Fig. 6b). The overall prediction error of a model based on FC is low (PE_{adj} = 36.96), as in previous studies, but the correlation between the residuals of the FC model and FC RI is strongly linear (Fig. 6b). Indeed, there is a stronger correlation between the residuals of the FC-based model and FC RI ($r^2 = 0.7191$) than between the residuals of the HBL model and FC RI ($r^2 = 0.4178$). In other words, BM estimates based on FC will vary by $\pm 26\%$ based on a single factor: how thick the animal's limbs are relative to its BM.

Moreover, this error is systematic rather than random: femur circumference overestimates BM in taxa with a very heavy body habitus (e.g., graviportal and fossorial taxa),

and the reverse is true for gracile and cursorial taxa. Notably, the relative degree of robustness (i.e., RI) cannot be predicted based on diaphyseal dimensions alone but must be determined relative to some other measurement of size (such as HBL or femur length). This is important because it is often assumed (but not tested) that most variation in mid-shaft dimensions/articular surface areas is explained by BM, and that midshaft dimensions/articular surface areas show little non-random variation independent of size due to their weight-bearing function (e.g., Alexander 1980; Anderson et al. 1985; Swartz 1989; Ruff 1990; Jungers 1990; Scott 1990; Anyonge 1993; Egi 2001; Campione and Evans 2012; however, these studies also note some of their taxa show systematic variation in the scaling of midshaft dimensions).

The effects and definition of "body habitus" are demonstrated more clearly in Fig. 7a, which illustrates two hypothetical species that are identical in all major linear proportions (i.e., they are scaled to the same HBL and have identical head, neck, and torso lengths, as well as identical axial lengths of the scapula, pelvis, and all major limb elements) but differ in body habitus as illustrated by girth and limb thickness. The blue (upper) species is cursorial, with a very gracile body habitus; its extremely slender limbs and neck are reminiscent of a chevrotain (Tragulidae), though it also resembles mammals with a long body and short neck such as mustelids, *Interatherium*, and *Hyopsodus*, which show the same types of errors as highly gracile mammals. Extant gracile mammals (e.g., many ruminants, canids) tend to have longer necks rather than longer torsos, but a longer torso is depicted here in order to keep head, neck, and torso proportions consistent between the two drawings. The purple (lower) species is very robust and reminiscent of a pygmy hippo (*Choeropsis liberiensis*) or a wombat (Vombatidae), with a large gut, deep skull, thick neck, and thick limbs (with correspondingly robust limb bones). It is evident that the more robust (purple) species will have a greater BM than the gracile (blue) one even though their HBL is the same. This discrepancy can be described as a difference in body habitus.

This same principle works in reverse for limb bone diameter and circumference. A limb bone of a given circumference could pertain to a very small individual of the robust species or a very large individual of the gracile one (Fig. 7b). Without another measure of size that is independent of either BM or bone circumference, such as HBL or bone length, there is no way to determine to which animal the bone pertains (and, therefore, to accurately predict its BM using only that variable). When using a measurement such as limb bone diameter or circumference to predict BM, it is generally assumed that this discrepancy does not matter: a large individual of a gracile species should have the same BM as a small individual of the robust species due to physical requirements imposed on FC by BM. The present study demonstrates that this is not the case; FC reflects

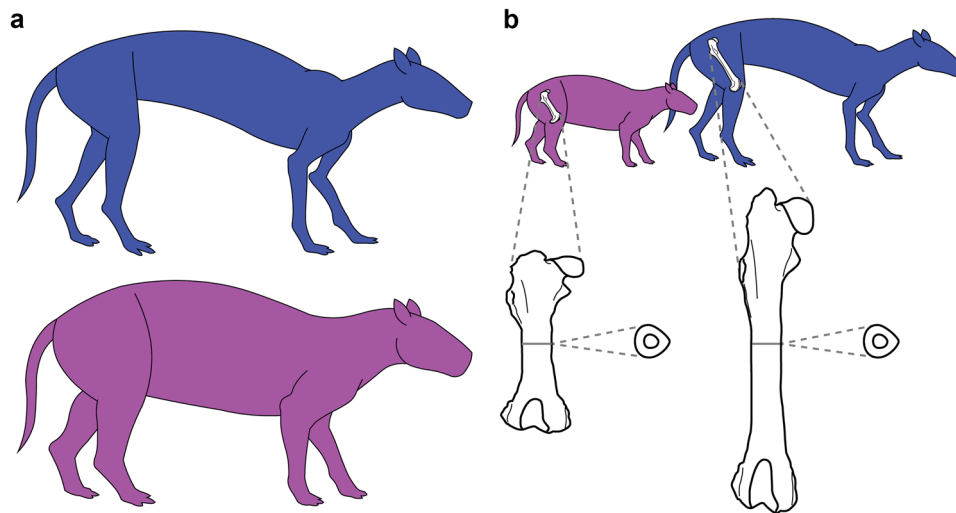


Fig. 7 Silhouettes of two hypothetical ungulate species, illustrating the effect of body habitus on body mass (BM) prediction: a very gracile ungulate (in blue), similar to a chevrotain (Tragulidae), and a very robust ungulate (in purple), similar to a pygmy hippo (*Choeropsis*) or a wombat (Vombatidae). In **a**, they are scaled to equal head-body length (HBL) and have equal limb, head, and neck lengths. Note that the purple species clearly has a greater BM than the blue spe-

cies, despite their equal HBL. In **b**, the individuals of the two species are scaled to have equal femur circumference (FC), illustrating that a femur of a given circumference could pertain to a smaller individual of the robust species (left) or a larger individual of the gracile species (right). As shown, despite equal femur dimensions, the blue species has a greater BM than the purple species

factors beyond BM, probably related to functional morphology and/or phylogenetic affinity. This can be deduced from Fig. 7b; if the individual of the more robust species were enlarged to the same BM as the individual of the more gracile species, it would have a greater FC rather than an equal one. The effects of body habitus on BM estimates tend to be negligible with generalized mammals but pronounced with very robust (e.g., fossorial or graviportal) or gracile (cursorial) taxa.

It is important to note body habitus is distinct from locomotor morphology. Although the most robust mammals (e.g., bears and elephants) tend to be plantigrade, and the most gracile mammals (e.g., some ungulates) tend to be unguligrade, body habitus refers to the overall shape of the body rather than the amount of mass concentrated in the distal limbs. For example, the rodent *Hydrochoerus hydrochaeris* and the artiodactyl *Sus scrofa* have very similar body plans; they are generalized terrestrial mammals with unspecialized limb proportions. However, *H. hydrochaeris* is plantigrade, whereas *S. scrofa* is unguligrade. These taxa show similar robustness indices based on femoral circumference (*H. hydrochaeris* = 5.39; *S. scrofa* = 5.31) and similar residuals (0.099 versus 0.089, respectively). Thus, these taxa have a similar body habitus despite their different limb morphologies.

Rather than reflecting limb morphology, body habitus reflects the width of the cylinders comprising the head + torso and limbs (sensu Prothero 1992) relative to their length. The robustness of the head, neck, and trunk appears to be

correlated with the robustness of the limbs, since limb mass and body mass scale isometrically in mammals (Kilbourne and Hoffman 2013); thus, mammals with reduced distal limb mass (cursorial taxa) do not have limbs that are overall less massive compared to generalized terrestrial taxa. Differences in distal limb morphology also would not explain why stylopodial measurements show a correlation with habitus, as differences in the mass of the distal limbs would not affect the amount of weight placed on the stylopodium and thus the relationship between stylopodial dimensions and BM. The graviportal taxa considered here have estimated weights only about half of their actual value, a discrepancy seemingly too great to be explained by thicker distal limb segments. These observations indicate that the relationship between body habitus and BM observed here cannot be explained solely by limb morphology.

The examples above suggest that the effects of body habitus should not be ignored when estimating BM, at least when using HBL or limb bone dimensions. To test this hypothesis, we created two models to estimate BM (one based on HBL, one based on FC) with FC RI (see Materials and methods) as an additional covariate as a proxy for body habitus. The variable FC RI has a significant effect on the %PE, %SEE, AIC, and BIC of the model, regardless of whether HBL ($t = 16.61, p < 0.001$) or FC ($t = -32.165, p < 0.001$) is the main predictor of BM (see Online Resource 3: Section 12). The effects of these models on BM estimates for notoungulates are discussed in the section below.

Notoungulate body mass estimates

Among the 14 species for which all three primary variables of interest could be measured (i.e., HBL, OCW, and CbL), none of these variables consistently yields higher or lower estimates than the others. For example, HBL predicts the lowest BM for three species, and the highest value for five species. Similar patterns characterize OCW and CbL BM estimates. This lack of a pattern has to do with systematic trends/biases in BM estimates noted in [Results](#).

Below, we integrate BM estimates for each species analyzed, compare our results to those of other studies, and provide a likely average BM range for each species. In general, ranges do not include values that appear to be outliers compared to other BM estimates, especially when such deviations match biases seen in extant mammals. For example, HBL tends to underestimate BM in extant large mammals with a robust body habitus. Therefore, HBL-based BM estimates for large, graviportal notoungulates were downweighted when considering a likely BM range if they could not be corrected for body habitus. In some cases, outlying BM estimates were downweighted when a posteriori examination revealed that the deviation was likely due to specimen distortion or incompleteness or inaccurate measurement, especially for specimens that could not be measured firsthand. In some cases, we used dental measurements or toothrow lengths as independent methods of estimating relative size of closely-related species (e.g., within the same subfamily) to help resolve conflicting BM estimates based on HBL, CbL, and/or OCW. Unlike cranial and skeletal measurements, tooth dimensions and toothrow lengths are commonly reported in the literature and are much less likely to suffer from preservational issues that result in inaccurate measurements. In addition, tooth dimensions are commonly used as a proxy for overall size in taxonomic diagnoses and to judge the range of size variation within a population (since teeth and dentitions are more common than other elements in the fossil record).

For some of the species we analyzed, many (> 20) BM estimates have been published. Most of these derive from two studies, Fariña et al. (1998) and Elissamburu (2010), which applied a wide variety of proxies and equations to a diversity of taxa. We do not discuss each of these BM estimates individually, as this would not only be unwieldy but also run counter to these studies, which focused on means and ranges of BM estimates. Instead, we combine these and other BM estimates graphically in histograms (Fig. 8) to illustrate the ranges and central tendencies of published BM estimates and variations between craniodontal and postcranial proxies. We discuss our results relative to the overall distributions of BM estimates and to results of other studies that have used more targeted approaches to determining body mass (e.g., Cassini et al. 2012a, b).

For our preferred BM estimates, we provide a range rather than a single value to account for individual BM variation within a population. To our knowledge, the only study that has examined this issue in mammals in general is that of Hallgrímsson and Maiorana (2000), who found that size variation increased with mean body mass. Those authors did not provide the primary data for their study, but their graphs suggest an average standard deviation in BM of ~12% for a 10-kg mammal and ~32% for a 100-kg mammal. The ranges we provide generally vary \pm 10–15% from their midpoint, similar to or perhaps a bit narrower than expected depending on the BM of the species in question.

We organize our discussion taxonomically, beginning with Toxodontia (proceeding upward from the base of the clade) and then discussing Typotheria. *Notostylops murinus* is discussed last; even though it likely diverged prior to the Toxodontia-Typotheria split (Cifelli 1993; Billet 2011), its BM could only be calculated based on limited data (CbL and OCW).

Isotemnidae

The three principal BM estimates for the late Eocene isotemnid toxodontian *Thomashuxleya externa* are rather divergent. However, these estimates derive from three specimens, and some of this variation is clearly intraspecific, since BM estimates based on CbL for two of these specimens differ by about 40% (98.4 kg vs. 137.1 kg; [Appendix](#)). For the smaller specimen (MPEF-PV 8166, the specimen described by Carrillo and Asher 2017), BM is estimated at 73.5 kg based on OCW. For the larger specimen (AMNH 28447), BM is estimated at 92.2 kg based on HBL of a composite specimen composed of it and a postcranium from the same site (AMNH 28906) that was partly reconstructed based on other basal toxodontians (see Shockley and Flynn 2007). However, this postcranium is likely too small to correspond to AMNH 28447 based on overlapping elements between it and MPEF-PV 8166; the length of the radius in the latter is 55% OCW (Carrillo and Asher 2017: table 4; [Appendix](#)), whereas it is 53% OCW in the two AMNH specimens (Shockley and Flynn 2007: table 1; [Appendix](#)). A correctly sized postcranium would result in a BM slightly greater than 92.2 kg for the composite AMNH skeleton based on HBL. When body habitus is considered, BM of the composite AMNH specimen is 105.3 kg based on HBL and 114.9 kg when based on femoral circumference (FC) (Table 3). Together, these data suggest a general BM range of 80–120 kg for *Thomashuxleya*. Our relatively low OCW BM estimate may be due to an inaccurate measurement since we were not able to study the specimen firsthand ([Appendix](#)), though it is only marginally below the BM range of 84 ± 24.2 kg of Carrillo and Asher (2017; see also Online Resource 5) based on the astragalus. A BM range of 80–120

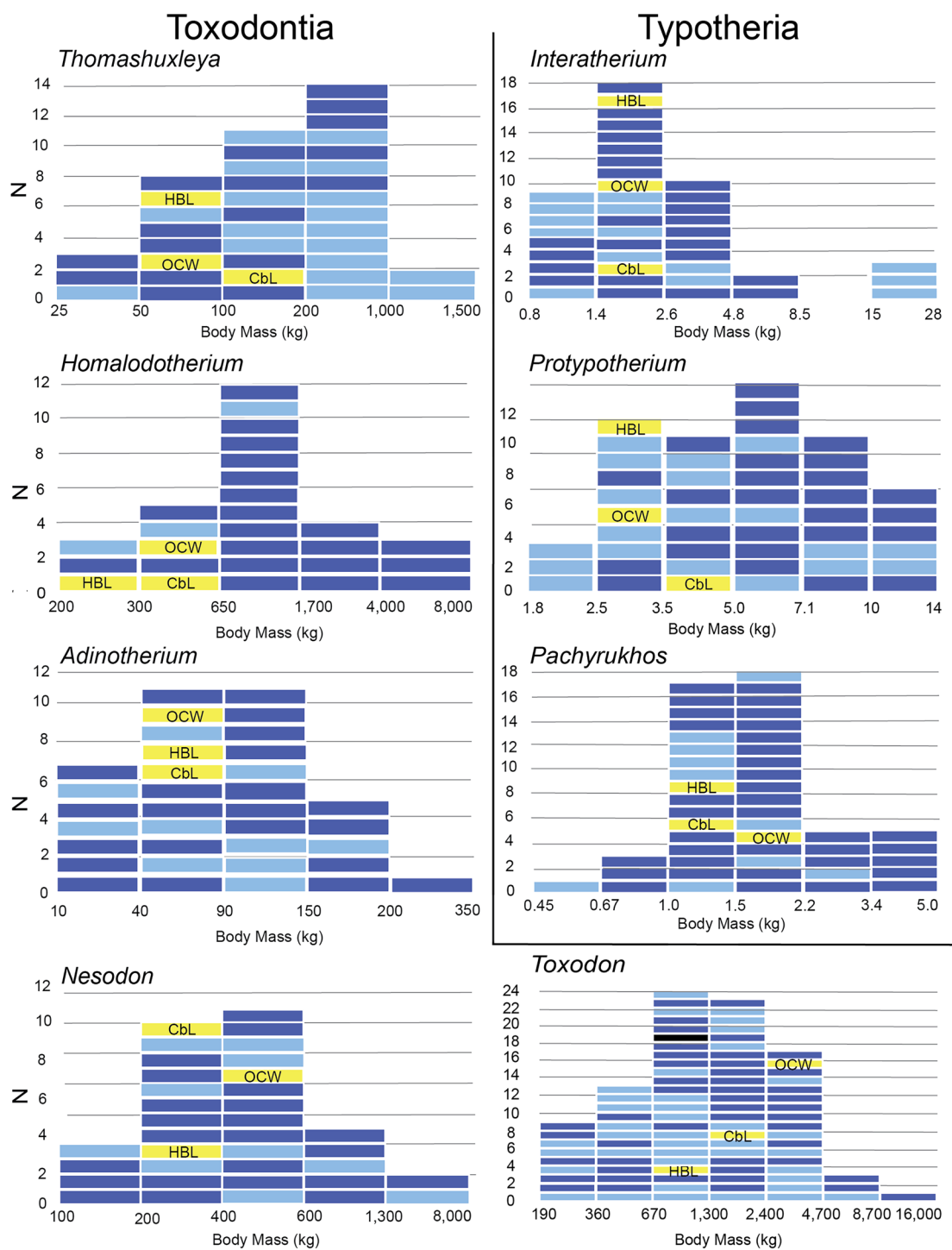


Fig. 8 Histograms showing body mass (BM) estimates for notoungulates for which more than 20 body mass estimates have been published. Each block represents a separate BM estimate. Estimates based on craniodental measurements are light blue, those based on postcranial measurements are in dark blue, a water displacement BM estimate is in black, and the estimates from this study are in yellow. Taxa are arranged in taxonomic order (top to bottom), to match the

text. Note that bin breadths are equal in terms of $\log_{10}(\text{kg})$ units; they appear unequal because they are presented in kg to facilitate comparisons with the text and published values. The original bin sizes and histograms (in \log_{10} units) are presented in Online Resource 6. Abbreviations: CbL, condylobasal length; HBL, head-body length; OCW, occipital condyle width

kg for *Thomashuxleya externa* is lower than most previous estimates for this notoungulate (Fig. 8) and overlaps the upper range of 70–90 kg published by Croft (2016: p. 59) for *T. rostrata*. It spans the BM estimate of 113 kg from Croft (2000: appendix 5.2) based on first upper molar (M1) length.

Homalodotheriidae

For the relatively large early Miocene toxodontian *Homalodotherium cunninghami*, HBL, CbL, and OCW BM estimates range from 202.7 kg (HBL) to 360.4 kg (OCW) (Table 3). Considering the tendency of HBL to produce relatively low BM estimates for large notoungulates and for OCW to produce relatively high estimates, the intermediate value based on CbL (305 kg) may be the most accurate of the three. Curiously, when body habitus is considered, BM based on HBL triples (1028.5 kg). Conversely, BM based on FC adjusted for body habitus is quite low (205.7 kg), very close to the original HBL BM estimate. (Body mass based simply on FC is nearly 4,000 kg; Online Resource 3: Table 12.3). *Homalodotherium* is unquestionably among the most aberrant notoungulates in terms of its postcranial morphology (Riggs 1937; Coombs 1983; Elissamburu 2010), and this likely accounts for these widely disparate estimates. Scott (1937: p. 519) compared *Homalodotherium* to a tapir in terms of overall size, and although this is only a “gestalt” estimate, it agrees with the range of 250–350 kg suggested in this study; the Brazilian tapir (*Tapirus terrestris*) has a BM of 208–233 kg in our dataset (Online Resource 1), and the Malayan tapir (*Acrocodia indicus*) is slightly larger (Khan 1997). Our estimated BM range is lower than most previously published estimates for *Homalodotherium*, nearly all of which exceed 500 kg and many of which exceed 1,000 kg (Fig. 8). An exception to this pattern is the estimate of 405 kg published by Cassini et al. (2012a). However, the concordance between this value and our estimates is likely coincidental, as this BM estimate is an average of ten craniodontal BM estimates that do not individually provide accurate BM estimates in other notoungulates (Online Resource 3). Interestingly, the 300 kg BM estimate of Croft (2000: appendix 5.2) for *Homalodotherium* based on M1 length is the midpoint of the BM range estimated here. The 350 kg estimate published by Vizcaíno et al. (2012: table 5.1) is at the upper end of our range, but the basis for this estimate was not specified.

The geologically youngest homalodotheriid, late Miocene *Chasicotherium rothi*, has been described as the largest member of the family (Bocchino de Ringuelet 1957). Our CbL measurements indicate that the skull of this species is about 10% larger than that of *Homalodotherium cunninghami*, but OCW values are nearly identical for these two species (Appendix). As a result, it is unclear if this species was

appreciably larger or not. This is supported by the limited postcranial measurements for *Chasicotherium rothi* published by Elissamburu (2012: appendix 1), which include values both larger and smaller than those for *Homalodotherium*. Considering the very limited material of *Chasicotherium* currently available (Elissamburu 2010), it is reasonable to assume a BM range broadly similar to that of *Homalodotherium* (i.e., 250–350 kg). This overlaps the lower part of the range of 315–500 kg published by Croft (2016: p. 171) based on rough estimates of HBL but is much smaller than the estimate of 1,116 kg published by Wilson et al. (2012: supp. table 1) based on lower first molar (m1) length.

Leontiniidae

For the large late Oligocene leontiniid toxodontian *Scarrittia canquelenensis*, mean BM based on CbL (495.8 kg) is about 20% greater than that based on HBL (418.4 kg). If the HBL estimate is adjusted for body habitus, it exceeds the mean CbL estimate by less than 10% (530.6 kg; Table 3) and is within the range of CbL estimates of the four specimens that were measured. Conversely, BM based on FC adjusted for body habitus is about 25% smaller than the unadjusted HBL estimate (333.2 kg; Table 3). We were unable to obtain OCW data for *Scarrittia*, but BM estimates based on other variables suggest a BM of around 450–550 kg. This is about one-third the average BM published for *Scarrittia* by Elissamburu (2012: table 2), which is based on a variety of postcranial and craniodontal measurements, and it is slightly smaller than values of 684 kg and 728 kg published by Wilson et al. (2012: supp. table 1) based on m1 length. Conversely, it is more than double the BM estimate of 208.6 kg published by Gomes Rodrigues et al. (2017: table S2) based on upper first molar (M1) length.

Body mass estimates for the late Oligocene leontiniid *Taubatherium paulacouti* based on HBL and CbL suggest this species was about one-third the size of *Scarrittia* (150–200 kg; Table 3). The three other leontiniids included in our study were between *Scarrittia* and *Taubatherium* in size based on CbL and OCW. Middle Miocene *Huilatherium pluriplicatum* was perhaps 10–15% smaller than *Scarrittia* (ca. 375–500 kg), slightly larger than the 280–370 kg estimate published by Croft (2016: p. 99). The two other late Oligocene leontiniids in our study, *Gualta cuyana* and *Leontinia gaudryi*, were likely in the 250–350 kg range (Table 3). This is compatible with the 288 kg estimate published by Vizcaíno et al. (2012: table 5.1) for *Leontinia* based on unspecified data. Our estimated range is roughly half the mean BM of 558 kg estimated for *Leontinia* by Elissamburu (2012: table 2), though it overlaps the lower part of the range if standard deviation is considered (270–846 kg). The relatively large OCW BM estimate for *Leontinia* in our study (65% greater than the CbL estimate) is likely due to an

inaccurate measurement, which was taken from the illustration of Loomis (1914: fig. 73).

Notohippidae

We measured several late Oligocene notohippids (*Eurygenium paceignum*, *Mendozahippus fierensis*, and *Rhynchippus equinus*), and most resulting BM estimates range from 40–50 kg (Table 3). The OCW estimate for *Rhynchippus* is slightly lower (32.0 kg), whereas the HBL BM for *Eurygenium paceignum* is much lower, only 13.4 kg. The latter is almost certainly due to inaccuracies in the skeletal reconstruction of Shockley (1997: fig. 5), which appears to have 5–6 cervical vertebrae, as opposed to the typical mammalian number of seven, and only 15 thoracolumbar vertebrae, in contrast to 19 or more in most placental mammals (Narita and Kuratani 2005; Sánchez-Villagra et al. 2007; Asher et al. 2011; Li et al. 2023). Together, our estimates suggest a typical BM range of 35–50 kg for these notohippids, less than half the BM estimated by Elissamburu (2012: table 2) for *Rhynchippus equinus* (ca. 85–115 kg) and about double the BM estimated by Croft (2000: appendix 5.2) for *Eurygenium paceignum* (21.3 kg). Our estimated BM range is slightly lower than BM estimate of 60 kg by Vizcaíno et al. (2012: table 5.1) for *Eurygenium*, *Rhynchippus*, and other notohippids based on analogy with extant *Ovis aries* (sheep).

Toxodontidae

Our BM estimates for the small early Miocene toxodontid notoungulate *Adinotherium ovinum* vary little, with the largest mean estimate (83.9 kg, based on OCW) only 12% greater than the smallest (74.9 kg, based on CbL; Table 3). This is likely due to the intermediate size of *Adinotherium* (i.e., near 100 kg), within the range of the BM distribution that tends to produce similar estimates for HBL and OCW. When the HBL estimate is adjusted for body habitus, it is only slightly greater than the mean OCW BM estimate (84.5 kg); body mass based on FC adjusted for body habitus is 92.4 kg (Table 3). Together, these suggest a BM range of about 75–90 kg for *Adinotherium*, slightly below the middle of the distribution of previously published BM estimates (Fig. 8; Online Resource 5). The BM estimates of Cassini et al. (2012a: Table 14.3) for both *Adinotherium ovinum* and *Adinotherium robustum* are beyond this range (100.29 kg and 126.24 kg, respectively), though the range of the former overlaps slightly when the standard deviation of 9.18 kg is considered. The opposite is true for the BM estimates of Cassini et al. (2012b: table 6), which are based on 3D cranium centroid size; their BM range for *Adinotherium robustum* (75.6–88.52 kg) overlaps our range for *A. ovinum*, but their range for *A. ovinum* (46.56–69.90 kg) does not. The 121 kg estimate for *Adinotherium* published

by Vizcaíno et al. (2012: table 5.1) is within the range of the Cassini et al. (2012a) estimate, about 50% larger than our estimated BM. Our BM estimates for early Miocene *Proadinothereum muensteri* based on CbL and OCW suggest a BM about twice that of *A. ovinum* (Table 3), compatible with a BM estimate of 130 kg published by Wilson et al. (2012: supp. table 1) based on m1 length.

Body mass estimates are more disparate for the medium-sized early Miocene toxodontid *Nesodon imbricatus*, with the largest mean BM estimate in our study (624.8 kg, based on OCW) more than double the smallest estimate (292.0 kg, based on HBL; Table 3). An intermediate mean value of 395.1 kg based on CbL is quite close to BM estimates adjusted for body habitus (363.3 kg and 390.3 kg based on HBL and FC, respectively; Table 3), suggesting a likely range of about 350–400 kg for *Nesodon imbricatus*. Like with *Adinotherium ovinum*, this is slightly below the midpoint of the range of previously published BM estimates for this species (Fig. 8; Online Resource 5). It is slightly higher than the 250–350 kg estimate of Croft (2016: p. 115) based on HBL. Estimates for two specimens of *N. imbricatus* by Cassini et al. (2012a; table 14.3) based on univariate craniodental measurements are slightly to much greater than ours (about 440–850 kg with standard deviations), whereas estimates of Cassini et al. (2012b: table 6) based on 3D cranium and mandible centroid size overlap this range (about 280–520 kg with standard deviations). Body mass estimates for *Nesodon taweretus* based on CbL and OCW indicate it may have been slightly smaller than *N. imbricatus* (Table 3).

The large Pleistocene toxodontid *Toxodon platensis* shows a pattern in BM estimates like that of smaller toxodontids but more extreme in terms of discrepancies among estimates. Mean BM based on OCW is unreasonably high (nearly 4,400 kg), roughly 6× that based on HBL (728.5 kg); mean BM based on CbL is intermediate (1,594.1 kg) but closer to the HBL estimate (Table 3). When the HBL is adjusted for body habitus, BM increases by about 20% (889.7 kg; Table 3). Body mass based on FC adjusted for body habitus is about 30% lower than this (630.9 kg; Table 3). Both of these body habitus-adjusted values are lower than the BM estimate of 1,100 kg calculated by Fariña and Alvarez (1994) based on water displacement of a scale model of *Toxodon platensis*. However, when the HBL measurement of Fariña et al. (1998: table 4) is adjusted for body habitus and used to estimate BM, the resulting value (1,168.9 kg) is remarkably close to the water displacement BM estimate of those authors. Fariña et al. (1998) generated 58 other BM estimates for *T. platensis* based on a wide variety of craniodental and postcranial measurements and calculated an arithmetic mean of 1,642 kg, a geometric mean of 1,187 kg, and a median value of 1,191 kg. In light of our analyses, a BM range of 1,000–1,200 kg for *Toxodon platensis* seems reasonable. Body mass estimates for the late Pleistocene toxodontid

Piauhytherium capivarae based on CbL and OCW would seem to suggest a BM of 1,000–2,000 kg (Table 3), but considering how these variables scale with BM in the larger *T. platensis*, a range of 700–800 kg is more likely. Similarly, late Pliocene to early Pleistocene *Charruatodoxodon uruguayensis* likely had a BM of 500–600 kg (Table 3).

Typotheria

Among typotheres, we were able to generate HBL, CbL, and OCW estimates for eight species, including four interatheriids (middle Eocene *Notopithecus adapinus*, early Miocene *Protypotherium australe*, early Miocene *Interatherium robustum*, and middle Miocene *Miocochilius anomopodus*), two mesotheriids (late Miocene *Plesiotypotherium achirense* and late Pliocene to Pleistocene *Mesotherium cristatum*), and two hegetotheriids (early Miocene *Pachyrukhos moyani* and Pliocene *Paedotherium typicum*). We calculated BM based on CbL and/or OCW for an additional 13 species in these families plus Archaeohyracidae.

Interatheriidae

Our BM estimates for the middle Eocene interatheriid *Notopithecus adapinus* suggest it is the second smallest species in our dataset. Body mass is estimated at 1.3 kg based on HBL and 1.1 kg based on CbL but a mere 0.5 kg based on OCW (Table 3). Considering that these three variables provide more concordant BM estimates in other small typotheres and that the CbL and OCW measurements are from the same specimen of *Notopithecus* (Appendix), the OCW estimate is probably anomalously low. A range of 1.0–1.5 kg is likely a reasonable average BM for the species. This is concordant with the 0.97–1.47 kg range published by Scarano et al. (2011: table 3) based on lower molar row length and slightly greater than the 800–1,000 g estimate published by Croft (2016: p. 61) based on first lower molar length. Vera (2017) calculated BM of *Notopithecus adapinus* based on several dental variables and measurements of the astragalus (using equations from Janis 1990, Scarano et al. 2011, and Tsubamoto 2014), and although the overall average (1.4 kg) is within the BM range proposed here, the different equations yielded results ranging from 0.67 kg to 1.82 kg (Vera 2017: table 3). The BM estimates of Wilson et al. (2012: supp. table 1) for *Notopithecus* based on m1 length span a range far beyond ours (0.7–5.2 kg).

Our mean BM estimates for *Interatherium robustum* based on HBL and OCW are within a very small range of 1.9–2.0 kg, and this is also true for HBL and FC BM estimates when adjusted for habitus (Table 3). The mean BM estimate based on CbL is about 20% lower (1.6 kg), perhaps due to the anteroposteriorly compressed skull of this species and other interatheriines (Sinclair 1909). These values

are near the middle of the range of previously published estimates (Fig. 8; Online Resource 5), including the 1–3 kg estimate of Croft (2016: p. 133), and overlap the BM ranges for this species published by Cassini et al. (2021a, b). The BM estimate of 1.25 kg published by Scarano et al. (2011) for *Interatherium rodens* is slightly below this range.

For *Protypotherium australe*, our BM based on HBL is similar to the mean value for CbL (3.5 kg and 3.7 kg, respectively), whereas the mean OCW estimate is about 25% smaller (2.8 kg; Table 3). When adjusted for body habitus, the HBL estimate equals the mean CbL estimate (i.e., it is 3.7 kg), and the FC estimate is about 10% greater (4.1 kg; Table 3). Thus, the average BM of *Protypotherium australe* was likely 3.5–4.0 kg, congruent with the 3D cranium centroid estimate of Cassini et al. (b: table 6) but more than 25% smaller than the mandible centroid estimate from the same study (4.93 kg). Our range is slightly lower than the estimate of Cassini et al. (2021a) based on univariate craniodental measurements (4.67–5.67 kg) and less than half their estimated range of 9.11–11.59 kg based on the multivariate equation of Mendoza et al. (2006), which is in the upper range of estimates for the genus (Fig. 8; Online Resource 5). The preferred estimates of Scarano et al. (2011: table 2) for *P. australe* are also slightly greater than our suggested BM range; these authors generated a mean BM of 5.86 kg and a maximum BM of 7.39 kg (excluding the 99% confidence interval). Other dental equations and datasets investigated by these authors yielded BM estimates ranging from about 1.4 kg to 21.4 kg (Scarano et al. 2011: table 3). Reguero et al. (2010) estimated the BM of *P. australe* at 2.8 kg, slightly below our BM range.

Curiously, our BM estimates for *Protypotherium praerutilum* show a pattern opposite that of *P. australe*, with the CbL BM estimate of 2.4 kg only about two-thirds that based on OCW (3.7 kg; Table 3). It is difficult to interpret these two values. However, the estimates of Scarano et al. (2011: table 2) suggest that this species was about 75% the size of *P. australe*, with a mean BM of 4.57 kg and a range of 3.87–5.8 kg. This would suggest a BM of about 2.5–3.0 kg based on our data for *P. australe*. Cassini et al. (2012b: table 6) estimated the BM of *P. praerutilum* at 2.38 kg based on cranium centroid size, very close this range. The 3.1 kg estimate of Cassini et al. (2021a: table 14.3) based on univariate regression equations of Janis (1990) is also quite close, but the 5.92 kg estimate from the same work based on the multivariate equation of Mendoza et al. (2006) is nearly twice as great.

Our body mass estimates for the middle Miocene interatheriid *Miocochilius anomopodus* are relatively disparate, ranging from 4.7 kg (based on OCW) to 10.9 kg (based on HBL; Table 3). Considering that BM based on CbL is 9.7 kg, close to the value based on HBL, the OCW value is likely erroneously low. Body mass estimates for

Miocochilius based on HBL and FC adjusted for body habitus (13.4 kg and 14.3 kg, respectively) are about one-third larger than estimates based on HBL and CbL. Kay and Madden (1997) placed *Miocochilius* in their 1–10 kg BM category, whereas Catena and Croft (2020) placed it in their 10–100 kg category, but neither work provided details of how BM was estimated. Our data concur with the latter study and suggest that this species had an average body mass slightly exceeding 10 kg, congruent with the estimate of Croft (2016: p. 145) of 11–13 kg based on HBL. Wilson et al. (2012: supp. table 1) estimated BM for 40 specimens of *Miocochilius* based on m1 length; the mean value of that sample (5.8 kg) is about half our estimate.

Mesotheriidae

Our BM estimates for the late Miocene mesotheriid *Plesiotypotherium achirense* range from about 30 kg (based on CbL and OCW) to about 40 kg (HBL; Table 3). We were unable to calculate an HBL estimate adjusted for body habitus without a value for femoral circumference, but these three values are relatively concordant even without such an adjustment. Our estimated range for *P. achirense* is about 1.5–2 × greater than estimates of ca. 20 kg calculated using M1 and m1 length and data from extant ungulates (Croft et al. 2004: table 13; Reguero et al. 2010: appendix 24.1). Conversely, our range is below the ca. 50–75 kg range for three specimens of *P. achirense* analyzed by Fernández-Monescillo et al. (2019: table 2) in which BM was calculated using craniodental equations. However, the raw BM estimates on which these average values are based span a considerably larger range (ca. 35–140 kg), even excluding ones that were discarded by these authors (Fernández-Monescillo et al. 2019: online resource 3: table 1). Wilson et al. (2012: supp. table 1) estimated the BM of the holotype of *P. achirense* at 58.6 kg based on m1 length, about 1.5–2 × our estimated BM range. We estimate that closely-related *Plesiotypotherium casirensis* had a BM about double that of *P. achirense*, 60–75 kg.

For late Pliocene to Pleistocene *Mesotherium cristatum*, our three BM estimates are remarkably consistent, differing by little more than 10% and suggesting a BM range of 90–110 kg (Table 3). Interestingly, the HBL estimate falls between the other two, even though it is only based on a rough estimate of HBL published by Bond (1999). Fernández-Monescillo et al. (2019: table 2) estimated the BM of *Mesotherium cristatum* at nearly 200 kg, about double the range suggested by our calculations. Croft et al. (2004: table 13) calculated a BM of *Mesotherium cristatum* at about 45 kg based on m1 length, though they calculated a BM of 65 kg for *Mesotherium cristatum* at about 45 kg based on m1 length, though they calculated a BM of 65 kg for *Mesotherium pachygnathum*, a species

now recognized as a junior synonym of *Mesotherium cristatum* (Fernández-Monescillo et al. 2022). Reguero et al. (2010: appendix 24.1) calculated a slightly greater BM for *Mesotherium cristatum* based on m1 length (73.4 kg). These dental values overlap the BM range of 58–67 kg published by Croft and Lorente (2021: S3 table) based on femur length and comparisons with a BM estimate of 24–28 kg published by Croft (2016: p. 101) for the late Oligocene mesothere *Trachytherus alloxus*.

We were able to calculate BM based on CbL and OCW for late Miocene *Typhotheriopsis chasicoensis*, and OCW yields a BM ca. 70% greater than that based on CbL (84.9 vs. 49.9 kg, respectively; Table 3). In this case, the OCW BM estimate is likely too great; comparison with our BM estimates for *Plesiotypotherium achirense*, which is only slightly smaller than *Typhotheriopsis chasicoensis* based on dental measurements (Croft et al. 2004: table 13), suggests a BM range of about 50–65 kg (Table 3). This is about double the 22–33 kg range published by Croft (2016: p. 173) based on estimated HBL, and more than double the estimate of 22.4 kg published by Croft et al. (2004: table 13) based on M1 length.

We calculated BM based on OCW for three other mesotheres, middle Miocene *Microtypotherium choquecotense* and two Pliocene species of *Pseudotypotherium* (*P. pulchrum* and *P. subinsigne*), though it is difficult to judge the accuracy of these values in the absence of CbL and HBL data for comparison. Our estimate of 13.5 kg for *Microtypotherium* (Table 3) is only slightly greater than the estimate of 11.6 kg published by Croft et al. (2004: table 13) based on M1 length and the estimate of 12.9 kg published by Reguero et al. (2010: appendix 24.1) based on m1 length. Thus, a BM of 10–15 kg seems reasonable for *Microtypotherium* in the absence of additional data.

Our BM estimate for Pliocene *Pseudotypotherium pulchrum* from Monte Hermoso based on OCW is 58.0 kg (Table 3), within the relatively large BM range of about 30–60 kg published by Croft et al. (2004: table 13) based on M1 length (but listed simply as *?Pseudotypotherium* sp.) and just slightly above the range of about 40–55 kg published by Reguero et al. (2010: appendix 24.1) based on M1 length for specimens identified as *Pseudotypotherium hystatum* and *Mesotherium maendrum* from this locality (both of which are now considered to pertain to *P. pulchrum*; Fernández-Monescillo et al. 2022). Considering that smaller specimens from these sites may represent juveniles, these values suggest a BM range of perhaps 45–65 kg. However, dental measurements of *Pseudotypotherium pulchrum* are greater than those of *Typhotheriopsis chasicoensis* (Croft et al. 2004: table 14.3), indicating that its BM should be greater than our 50–65 kg estimate for that species, perhaps 60–80 kg.

Our estimate for *Pseudotypotherium subinsigne* based on OCW is 140 kg (Table 3). However, this value that is likely too large considering that tooth dimensions of *P. subinsigne*

are similar to those of *Mesotherium cristatum*, a closely-related mesothere represented by more complete remains. For example, Rovereto (1914: p. 215) listed m1 length of *Pseudotylotherium subinsigne* at 24.0 mm, within the range of *Mesotherium cristatum* (Croft et al. 2004: table 13). In the absence of additional proxies for *P. subinsigne*, it is reasonable to assume a BM range similar to that of *Mesotherium* (i.e., 90–110 kg).

Archaeohyracidae

Definitive postcranial remains of archaeohyracids have yet to be identified (Croft et al. 2003; Shockley and Anaya 2008), so BM estimates for these species must be based on craniodental measurements. We generated BM estimates based on CbL and OCW for two species, early Oligocene *Archaeotylotherium tinguiriricaense* and late Oligocene *Archaeohyrax patagonicus*. For the former species, the two values are within nearly 5% of one another and suggest a BM of 3–4 kg (Table 3), very close to the 3.2 kg estimate of Croft (2000: appendix 5.1, listed as gen. et sp. nov. A) based on M1 length but much smaller than the 8.3–8.6 kg BM estimates of Wilson et al. (2012: supp. table 1) based on m1 length. Considering the CbL of *Archaeotylotherium* is within the range of variation observed for the interatheriid *Prototylotherium australe* (Appendix), whose BM is estimated at 3.5–4.0 kg based on several independent variables (including FC adjusted for body habitus), BM estimates for *Archaeotylotherium* based on m1 length appear to be overestimates.

Our two BM estimates for *Archaeohyrax patagonicus* are greater and more divergent from one another than those for *Archaeotylotherium tinguiriricaense*, suggesting a BM range of perhaps 9–13 kg (Table 3). This is much greater than the 2.8 kg estimate published by Reguero et al. (2010) was from a highly worn upper molar, since the anteroposterior dimension of archaeohyracid upper molars decreases substantially with wear (Croft et al. 2003; Billet et al. 2009). This inference is supported by the fact that much greater BM estimates for this species are generated based on m1 length; BM values for *Archaeohyrax patagonicus* from Wilson et al. (2012: supp. table 1) range from 10.8–16.2 kg, mostly overlapping the BM range suggested by our data.

Hegetotheriidae

The two hegetotheriids for which HBL, CbL, and OCW could be measured both pertain to the subfamily Pachyrukhinae: early Miocene *Pachyrukhos moyani* and Pliocene *Paedotherium typicum*. Average BM estimates for *Pachyrukhos moyani* based on these variables, as well as BM estimates based on HBL and FC adjusted for body habitus, are between 1.2 and 1.6 kg (Table 3). When adjusted for body habitus,

BM estimates based on HBL and FC are also within this range (1.3 and 1.4 kg, respectively). This suggests an average BM range of 1.2–1.6 kg for *Pachyrukhos moyani*, which has the same relationship to values published by Cassini et al. (2012a, b) as those for *Prototylotherium australe* discussed above; our range brackets the mean value of 1.56 kg published by Cassini et al. (2012b: table 6) based on cranium centroid size, it is slightly below the 1.62 kg value published by Cassini et al. (2012a: table 14.3) based on univariate equations of Janis (1990), and it is less than two-thirds the BM predicted by Cassini et al. (2012a: table 14.3) based on the multivariate equation of Mendoza et al. (2006). Our estimated BM range for *Pachyrukhos moyani* is slightly below the midpoint of the distribution of previously published estimates for this species (Fig. 8; Online Resource 5).

Our BM estimates for *Paedotherium typicum* span a larger range than those for *Pachyrukhos moyani*, from 1.4 kg to 2.4 kg, with CbL and OCW yielding the smallest estimates and HBL yielding the largest (Table 3). As for *Pachyrukhos moyani*, HBL and FC values fall within this range when adjusted for body habitus (2.1 kg in both cases). *Paedotherium typicum* was probably slightly larger than *Pachyrukhos* based on its larger skull, which suggests a BM range of 1.6–2.4 kg. This is broadly congruent with the BM range of ca. 1.5–2.8 kg for *Paedotherium typicum* published by Elissamburu and Vizcaíno (2005: appendix 1) based on several measurements of the humerus and femur but mostly below the range of ca. 2.3–2.8 kg published by Elissamburu (2004: appendix 3) based on a broader sample of postcranial and craniodental measurements. It is slightly greater than the 1–2 kg estimate of Croft (2016: p. 215) based on head-body length.

Our BM estimates for closely-related *Paedotherium bonaerense*, which are only based on CbL and OCW, show an opposite relationship to corresponding values for *Paedotherium typicum*, with the value based on CbL (1.5 kg) exceeding that based on OCW (1.1 kg; Table 3). At face value, these would suggest a BM range of about 1.0–1.5 kg. However, *P. bonaerense* is close in size to *P. typicum*, less than 5% smaller based on linear toothrow measurements (Cerdeño and Bond 1998: table 3). Assuming geometric similarity, this suggests an average BM about 10–15% smaller (1.4–2.0 kg). The discrepancy between this range and our OCW BM estimate could be due to a mismeasurement, since the specimen was not studied firsthand. Our estimated BM range for *P. bonaerense* is much larger than the 340 g estimate published by Reguero et al. (2010: appendix 24.1) for this species based on M1 length but is close to the mean value of just over 2 kg published by Elissamburu (2012: table 2).

Body mass estimates for the Pliocene pachyrukhine *Tremacyllus intermedius* based on CbL and OCW yield the same value of 0.6 kg (Table 3). This species is about 25% smaller than *Paedotherium typicum* based on linear toothrow

measurements (Cerdeño and Bond 1998: tables 3, 8), which suggests a BM range of 0.6–1.0 kg based on geometric similarity, roughly congruent with our CbL and OCW estimates. As for *Paedotherium bonaerense*, this range is much greater than the 224 g BM estimate for *Tremacyllus* published by Reguero et al. (2010: appendix 24.1) based on M1 length. It is slightly below the mean value of 1.2 kg published by Elissamburu (2012: table 2) for this species.

We generated BM estimates based on HBL and CbL for the late Oligocene pachyrukhine *Prosotherium garzoni* of 2.0 and 4.0 kg, respectively (Table 3). The large difference between these values may be partly due to an underestimate of HBL; the value was measured from skeleton in which a portion of the vertebral column was not preserved (Appendix), and although Simpson (1945) endeavored to reconstruct the missing portions correctly based on other notoungulates, the result appears to have atypical proportions. Wilson et al. (2012: supp. table 1) published BM estimates for five specimens of *Prosotherium garzoni* based on m1 length, and the resulting values (1.8–3.7 kg; mean = 2.7 kg) suggest a BM near the midpoint of our two estimates. This contrasts with the much smaller value of 644 g calculated by Reguero et al. (2010: appendix 24.1) based on M1 length. Elissamburu (2012: table 2) estimated BM for two specimens of *Prosotherium garzoni* (sensu Seoane et al. 2017) at about 2–3 kg based on craniodental values. We estimate an average BM range of 2.5–4.0 kg for the species.

We were able to generate BM estimates for two non-pachyrukhine (i.e., hegetotheriine) hegetotheriids based on CbL and OCW: early Miocene *Hegetotherium mirabile* and middle Miocene *Hemihegetotherium trilobus*. For *Hegetotherium*, both variables generated a BM estimate of 4.9 kg (Table 3). This is close to the estimate of 4.67 kg published by Cassini et al. (2012b: table 6) based on cranium centroid size and about 25% smaller than their estimate of 6.42 kg based on mandible centroid size. Estimates of Cassini et al. (2012a: table 14.3) are higher still: 7.20 kg based on univariate regression equations and 8.21 kg using a multivariate regression equation. The BM estimate of 2.1 kg of Croft (2000: appendix 5.1) based on M1 length is about half that predicted here, as is the 2.2 kg estimate of Reguero et al. (2010: appendix 24.1) based on m1 length. Conversely, Wilson et al. (2012: supp. table 1) generated significantly larger BM estimates of 5.7 and 6.2 kg for *Hegetotherium mirabile* based on m1 length. We estimate the average BM of the species at 4.5–5.5 kg.

Body mass estimates for *Hemihegetotherium trilobus* are greater and slightly less congruent than those for *Hegetotherium*: 9.3 kg based on CbL and 10.4 kg based on OCW (Table 3). Solórzano and Núñez-Flores (2021: table S6) estimated the body mass of this species at 11.5 kg based on several dental measurements, and Wilson et al. (2012:

supp. table 1) estimated the BM of three specimens at 8.0–11.2 kg (mean = 9.2 kg) based on m1 length. Together, these suggest an average BM of 9–12 kg, within the range of the 9–17 kg BM estimate of Croft (2016: p. 159) based on approximate HBL.

As indicated at the beginning of this section, we were only able to generate BM estimates for the early-diverging notoungulate *Notostylops murinus* (Notostylopidae) based on CbL and OCW. These vary by about one-third, with CbL yielding a BM estimate of 4.0 kg and OCW generating a BM estimate of 2.7 kg. Previously-published BM estimates for *Notostylops* span more than an order of magnitude. Croft (2000: appendix 5.1) calculated its BM at 3.1 kg based on M1 length, while Elissamburu (2012: table 2) calculated its BM at 11.9 kg based on several dental measurements. Croft (2016: p. 67) used remains of *Notostylops* and approximate HBL calculations to estimate the BM of the similarly-sized *Otronis muhlbergi* at 6–9 kg. Berqvist and Metello (2011) estimated the BM of *Notostylops* at 7–55 kg based on various humerus and femoral measurements, while Vizcaíno et al. (2012: table 5.1) estimated its BM at 50 kg based on analogy with extant *Ovis aries* (sheep). Most recently, Lorente et al. (2019) estimated the BM of *Notostylops murinus* at about 5–14 kg based on measurements of the astragalus. Considering that the cranium analyzed in our study is a juvenile (Simpson 1948), it is reasonable to assume that it lies at the low end of the size spectrum, leading us to estimate an average BM for the species of perhaps 4–10 kg.

Conclusions

A significant and rather unexpected result of our analysis of extant mammals is the effect that body habitus can have on body mass estimates. Our data indicate that its effects are independent of body size (BM), vary systematically across mammals (i.e., its effects are not confined to a single clade), and can produce large errors in particularly robust (e.g., graviportal) or gracile (e.g., cursorial) mammals. Quantifying and attempting to correct for body habitus of extinct mammals, as we have done here, can be challenging, even when relatively complete remains are available. However, not accounting for habitus can result in what are likely inaccurate BM estimates. This concern is especially relevant to estimates based on postcranial variables, which are typically considered to be largely independent of variables other than size. It is possible that many mammal BM estimates based on postcranial proxies are not accurate and should be re-evaluated using additional types of evidence. Among notoungulates, the effect of body habitus is greatest in large toxodontians such as *Homalodotherium*, *Scarrrittia*,

and *Toxodon*, in which FC-based BM estimates are 2–18× greater when body habitus is considered as a covariate.

In extinct clades such as notoungulates that lack close living relatives, focusing on a limited number taxa known from relatively complete skeletons is an advisable first step for attempting to infer BM of any member of the group. With relatively complete remains, several independent or semi-independent approaches for BM inference can be used to generate high-confidence BM ranges for well-known species. Such species can then be used as “calibration points” for determining the relationship between BM and other variables (e.g., lower molar length) in the group, allowing BM of species known from more limited remains to be estimated with greater confidence. Among notoungulates, the most appropriate taxonomic level for such comparisons is likely the family, as members of a family tend to be consistent in overall morphology. For early-diverging species and members of paraphyletic families, a broader sample may be required. Our study suggests that molar length can be used to generate accurate BM estimates for some notoungulates, but care should be taken with this approach, as it can vary by group or species, particularly those with hypsodont teeth in which tooth dimensions change with wear. Additionally, the accuracy of this proxy can only be gauged by comparing dental estimates with those based on other types of data.

Studies of other large extinct vertebrates (e.g., Gunga et al. 2008; Bates et al. 2015; Brassey et al. 2015; Hart et al. 2022) have used physical or digital life reconstructions to infer body mass. This method has been applied less frequently to mammals than to most other extinct organisms (especially dinosaurs; Brassey 2016), though some studies have applied this to fossil mammalian taxa (Sellers et al. 2012; Basu et al. 2016; Brassey et al. 2018; Rovinsky et al. 2020; Romano et al. 2021). Our analysis of *Toxodon platensis* suggests that such models may provide another useful BM datapoint for other mammals despite the assumptions about soft tissue reconstruction that must be made to undertake such reconstructions. This may be because the soft tissue anatomy of extinct mammals can be more easily constrained than in most other groups of extinct vertebrates.

Our study does not support the hypothesis that notoungulates generally have disproportionately large heads, at least as measured by CbL. However, a relatively large head does seem to characterize the late Pleistocene toxodontid *Toxodon platensis*. Apparent overestimates of BM in other large notoungulates based on craniodental variables could be due to notoungulate skulls being larger than most extant ungulates in other dimensions such as depth, which could be related to the development of hypselodont dentitions in most Neogene lineages. The fact that BM estimates based on cranium centroid size (Cassini et al. 2012b) are more compatible with our estimates than those based on linear measurements (Cassini et al. 2012a) supports the idea that only certain cranial dimensions are disproportionately large in some notoungulates.

Although we have generated what we consider to be reliable BM estimates for most groups of notoungulates that are represented by virtually complete skeletons, we were not able to calculate BM estimates adjusted for body habitus for any mesotheres due to a lack of circumference measurements. Considering the very broad range of BM estimates for mesotheres that have been published and their apparently robust body habitus (potentially similar to wombats; Shockley et al. 2007), this is one area where additional investigation is needed.

Perhaps the greatest takeaway from our study is that no anatomical proxy shows a perfect correlation with size/body mass. Even dimensions of limb bones that are closely associated with weight-bearing exhibit some non-random variation independent of body mass. Given this, researchers should carefully consider what variable(s) can best be used to represent size in their analysis, taking into account the characteristics of the taxon under consideration, the material available for study, and any potentially confounding specializations. When inferring body mass of extinct species, there will inevitably be at least one taxon that apparently breaks the rules of morphological scaling. Using multiple approaches to estimate body mass that are relatively independent of one another increases the chances of recognizing such taxa and thereby opening up new investigations into the particular features that make it an outlier.

Appendix

Measurement data, source(s), and body mass estimates (in kg) for notoungulate specimens analyzed in this study. Species are listed alphabetically within each family, and families are ordered phylogenetically. Specimens of the same species are ordered by collection number. Column abbreviations: **BM**, body mass; **CbL**, condylosal length; **HBL**, head-body length; **M**, measurement; **OCW**, occipital condyle width; **PI**, prediction interval. Family abbreviations: **Arc**, Archaeohyracidae; **Heg**, Hegetotheriidae; **Hom**, Homalodotheriidae; **Int**, Interatheriidae; **Iso**, Isotemnidae; **Leo**, Leontiniidae; **Mes**, Mesotheriidae; **Nth**, Notohippidae; **Nts**, Notostylopidae; **Tox**, Toxodontidae

Species	Family	Specimen	CbL	HBL				OCW			Source(s)
				M (mm)		BM	95% PI	M (cm)		BM	95% PI
				M	mm			M	cm		
TOXODONTIA											
<i>Notiosloops murinus</i>	Nts	FMNH PM 13319	100.8	4.0	(1.6–10.0)	–	–	–	–	20.7	2.7
<i>Thomashuxleya externa</i> ^a	Iso	AMNH 28447	312.9	137.1	(54.0–348.0)	–	–	–	–	–	—
<i>Thomashuxleya externa</i> ^a	Iso	AMNH 28447, 28905	–	–	—	144.8	92.2	(47.0–181.0)	–	–	—
<i>Thomashuxleya externa</i> ^b	Iso	MPEF-PV 8166	280.0	98.4	(38.8–249.8)	–	–	–	54.3	73.5	(37.1–145.5) Carrillo and Asher (2017: fig. 2); photos by Carrillo pers. comm
<i>Chasicotherium rothi</i>	Hom	MLP 26-XI-20-1	452.7	403.2	(158.5–1025.3)	–	–	–	89.3	360.1	(181.6–714.2) Bocchino de Ringuelet (1957: pl. 1)
<i>Homalodotherium cunninghami</i>	Hom	FMNH PM 13092	411.0	305.0	(120.0–775.3)	188.7	202.7	(103.2–398.0)	89.3	360.4	(181.7–714.7) Riggs (1937: fig. 55)
<i>Gualia cuyana</i>	Leo	MCNAM-PV 3951	386.0	254.2	(100.0–645.8)	–	–	–	85.4	313.2	(158.0–621.1) Cerdeño and Vera (2015: tab. 1, figs. 2–3)
<i>Huiatherium plurippicatum</i>	Leo	UCMP 39961	457.8	416.4	(163.7–1058.9)	–	–	–	96.9	465.2	(234.5–922.8) Villarroel and Colwell Danis (1997: fig. 19.1)
<i>Leontinia gaudryi</i>	Leo	AC 3292	392.0	265.8	(104.6–675.6)	–	–	–	95.1	439.0	(221.3–870.9) Loonius (1914: fig. 73)
<i>Scarritita canquensis</i>	Leo	AMNH 29571	464.0	432.8	(170.2–1100.7)	240.7	418.4	(213.1–821.7)	–	–	— Chaffee (1952: pl. 8)
<i>Scarritita canquensis</i>	Leo	AMNH 29578	431.0	350.0	(137.7–889.7)	–	–	–	–	–	— Chaffee (1952: p. 532)
<i>Scarritita canquensis</i>	Leo	AMNH 29581	533.0	642.9	(252.6–1636.0)	–	–	–	–	–	— Chaffee (1952: pl. 10)
<i>Scarritita canquensis</i>	Leo	USNM 13879	507.0	557.6	(219.2–1418.8)	195.0	223.8	(114.0–439.3)	–	–	— Chaffee (1952: pl. 7)
<i>Taubatherium paulacoutoi</i>	Leo (Composite)	346.4	185.1	(72.9–470.0)	175.2	162.5	(82.8–318.9)	68.8	157.6	(79.5–312.3) Couto-Ribeiro (2015: fig. 64)	
<i>Eurygenium pacceum</i>	Nth	Reconstruction	221.4	48.4	(19.1–122.7)	75.8	13.4	(6.8–26.3)	–	–	— Shockley (1997: fig. 5)
<i>Mendozahippus ferensis</i> ^c	Nth	MCNAM-PV 4004, 3846	211.0	41.7	(16.5–105.8)	–	–	–	48.0	49.1	(24.8–97.1) Cerdeño and Vera (2010: fig. 2)
<i>Rhynchoshippus equinus</i>	Nth	MPEF-PV 695	219.0	46.8	(18.4–118.6)	–	–	–	42.2	32.0	(16.2–63.4) Martínez et al. (2016: tab 2, figs. 2, 9)

Species	Family	Specimen	CbL			HBL			OCW			Source(s)	
			M (mm)	BM	95% PI	M (cm)	BM	95% PI	M (mm)	BM	95% PI		
<i>Adinotherium ovinum</i>	Tox	YPM VPPU 15003	-	-	-	-	-	-	51.0	59.9	(30.2–118.5)	Scott (1912: p. 226)	
<i>Adinotherium ovinum</i>	Tox	YPM VPPU 15118	256.0	75.2	(29.6–190.7)	-	-	-	59.0	96.3	(48.6–190.6)	Scott (1912: p. 226)	
<i>Adinotherium ovinum</i>	Tox	YPM VPPU 15131 (mostly)	253.0	72.5	(28.6–184.0)	136.5	77.3	(39.4–151.7)	54.0	72.2	(36.5–142.9)	Scott (1912: p. 226, and Pl. XII)	
<i>Adinotherium ovinum</i>	Tox	YPM VPPU 15382	258.0	77.0	(30.3–195.3)	-	-	-	61.0	107.2	(54.1–212.3)	Scott (1912: p. 226)	
<i>Nesodon imbricatus</i>	Tox	AMNH 9234	425.0	336.1	(132.2–854.4)	-	-	-	94.4	428.8	(216.2–850.5)	Present study	
<i>Nesodon imbricatus</i>	Tox	(Composite)	438.6	368.1	(144.8–935.8)	213.3	292.0	(148.7–573.4)	-	-	-	Scott (1912: pl. XII)	
<i>Nesodon imbricatus</i>	Tox	YPM VPPU 437.0	364.2	(143.2–926.0)	-	-	-	98.0	481.8	(242.9–955.9)	Scott (1912: p. 187)		
<i>Nesodon imbricatus</i>	Tox	YPM VPPU 15000	478.0	471.3	(185.3–1198.7)	-	-	-	127.0	1072.0	(539.8–2128.8)	Scott (1912: p. 187)	
<i>Nesodon imbricatus</i>	Tox	YPM VPPU 15141	442.0	376.4	(148.0–956.9)	-	-	-	96.0	451.8	(227.8–896.3)	Scott (1912: p. 187)	
<i>Nesodon imbricatus</i>	Tox	YPM VPPU 15256	472.0	454.5	(178.7–1156.1)	-	-	-	110.0	689.4	(347.3–1368.2)	Scott (1912: p. 187)	
<i>Nesodon imbricatus</i>	Tox	MHNNSR-PV 15336	440.0	371.5	(146.1–944.5)	-	-	-	105.0	597.0	(300.8–1184.6)	Forasiepi et al. (2015: fig. 3)	
<i>Nesodon taverensis</i>	Tox	1004	FC-DPV-514	502.0	542.1	(213.1–1379.2)	-	-	145.1	1608.6	(809.5–3196.4)	Ferrero et al. (2022: figs. 3–5)	
<i>Charruatoxodon uruguayanus^d</i>	Tox	FUMDHAM 48947	-	-	-	-	-	-	162.0	2242.3	(1127.9–4457.9)	Guérin and Faure (2013: tab. 1)	
<i>Piaytherium capivarae</i>	Tox	FUMDHAM 108998	-	-	-	-	-	-	155.0	1963.0	(987.6–3901.8)	Guérin and Faure (2013: tab. 1)	
<i>Piaytherium capivarae</i>	Tox	FUMDHAM 185391	664.0	1193.1	(468.3–3039.8)	-	-	-	151.0	1814.0	(912.8–3605.2)	Guérin and Faure (2013: tab. 1)	
<i>Piaytherium capivarae</i>	Tox	FUMDHAM 188265	628.0	1020.9	(400.8–2600.3)	-	-	-	164.0	2326.6	(1170.2–4625.7)	Guérin and Faure (2013: tab. 1)	
<i>Proadinothereum muensteri</i>	Tox	FMNH PM 13590	316.0	141.1	(55.6–358.4)	-	-	-	71.5	178.1	(89.9–353.0)	Hernandez del Pino (2018: fig. 4)	
<i>Toxodon platensis</i>	Tox	AMNH 11169	762.4	1750.6	(686.6–4463.6)	-	-	-	210.6	4904.8	(2464.0–9763.4)	Present study	
<i>Toxodon platensis</i>	Tox	FUMDHAM 186001	710.0	1437.6	(564.0–3664.0)	-	-	-	195.0	3903.1	(1961.5–7766.6)	Guérin and Faure (2013: tab. 1)	
<i>Toxodon platensis</i>	Tox	(Reconstruction)	-	-	-	290.0	728.5	(370.9–1430.8)	-	-	-	Farfia et al. (1998: tab. 4)	

Species	Family	Specimen	ChL			HBL			OCW			Source(s)	
			M (mm)	BM	95% PI	M (cm)	BM	95% PI	M (mm)	BM	95% PI		
TYPOTHERIA													
<i>Interatherium robustum</i>	Int	AMNH 9154	72.3	1.3	(0.5–3.3)	—	—	—	18.4	1.8	(0.9–3.6)	Present study	
<i>Interatherium robustum</i>	Int	AMNH 9263	82.8	2.0	(0.8–5.2)	—	—	—	18.9	2.0	(1.0–3.9)	Sinclair (1909: pl. VIII, figs. 16, 19)	
<i>Interatherium robustum</i>	Int	AMNH 9273	81.8	2.0	(0.8–5.0)	—	—	—	19.3	2.1	(1.1–4.2)	Present study	
<i>Interatherium robustum</i>	Int	AMNH 9299	72.0	1.3	(0.5–3.2)	—	—	—	19.1	2.1	(1.0–4.1)	Present study	
<i>Interatherium robustum</i>	Int	YPM VPPU 15041	74.8	1.4	(0.6–3.7)	—	—	—	17.2	1.4	(0.7–2.8)	Sinclair (1909: pl. VIII, figs. 17–18)	
<i>Interatherium robustum</i>	Int	YPM VPPU 15401, 15348	—	—	—	40.1	2.0	(1.0–4.0)	—	—	—	Sinclair (1909: pl. IX)	
<i>Miocochilus anomopodus^a</i>	Int	AMNH uncatalogued	133.7	9.9	(3.9–25.2)	70.6	10.9	(5.5–21.3)	21.8	3.3	(1.7–6.5)	Present study	
<i>Miocochilus anomopodus</i>	Int	MHNT-VPPLT 130.6	9.2	(3.6–23.4)	—	—	—	—	—	—	—	Present study	
<i>Miocochilus anomopodus</i>	Int	MHNT-VPPLT 982 MT	7.5	(3.0–18.9)	—	—	—	—	25.5	5.7	(2.9–11.4)	Present study	
<i>Miocochilus anomopodus</i>	Int	MHNT-VPPLT 1512	122.4	—	—	—	—	—	—	—	—	Present study	
<i>Miocochilus anomopodus</i>	Int	MHNT-VPPLT 1681 MT	128.4	8.7	(3.4–22.1)	—	—	—	25.6	5.8	(2.9–11.5)	Present study	
<i>Miocochilus anomopodus</i>	Int	IGM 182803	137.1	10.8	(4.3–27.3)	—	—	—	23.4	4.2	(2.1–8.3)	Present study	
<i>Miocochilus anomopodus</i>	Int	UCMP 38409	138.5	11.1	(4.4–28.2)	—	—	—	23.5	4.3	(2.2–8.5)	Stirton (1953: pl. X)	
<i>Miocochilus anomopodus</i>	Int	UCMP 39092	129.8	9.0	(3.6–22.9)	—	—	—	24.0	4.7	(2.4–9.2)	Present study	
<i>Miocochilus anomopodus</i>	Int	UCMP (Multiple)	—	—	—	72.5	11.8	(6.0–23.1)	—	—	—	Stirton (1953: pl. VIII)	
<i>Miocochilus anomopodus</i>	Int	AMNH 28949	68.2	1.1	(0.4–2.7)	—	—	—	12.8	0.5	(0.2–0.9)	Simpson (1967: fig. 23)	
<i>Miocochilus anomopodus</i>	Int	(Reconstruction)	—	—	—	34.8	1.3	(0.7–2.6)	—	—	—	Vera (2012: fig. 7)	
<i>Notopithecus adainus</i>	Int	AMNH 9226	103.8	4.4	(1.7–11.0)	—	—	—	21.3	3.0	(1.5–6.0)	Present study	
<i>Notopithecus adainus</i>	Int	AMNH 9260	98.7	3.7	(1.5–9.3)	—	—	—	21.3	3.0	(1.5–6.0)	Present study	
<i>Protopotherium australe</i>	Int	AMNH 9286	102.7	4.2	(1.7–10.7)	—	—	—	19.7	2.3	(1.2–4.5)	Present study	
<i>Protypotherium australe</i>	Int	AMNH 9334	97.1	3.5	(1.4–8.9)	—	—	—	21.1	2.9	(1.5–5.8)	Present study	
<i>Protypotherium australe</i>	Int	AMNH 9486	—	—	—	—	—	—	19.4	2.2	(1.1–4.3)	Present study	
<i>Protypotherium australe</i>	Int	AMNH 9556	—	—	—	—	—	—	19.9	2.4	(1.2–4.7)	Present study	
<i>Protypotherium australe</i>	Int	AMNH 9565	102.3	4.2	(1.6–10.5)	—	—	—	22.1	3.4	(1.7–6.8)	Sinclair (1909: pl. III, fig. 4)	
<i>Protypotherium australe</i>	Int	FMNH PM 13235	96.4	3.4	(1.3–8.6)	—	—	—	21.0	2.9	(1.5–5.7)	Present study	
<i>Protypotherium australe</i>	Int	(Reconstruction)	90.1	2.7	(1.1–6.9)	48.2	3.5	(1.8–6.8)	—	—	—	Sinclair (1909: pl. VII)	
<i>Protypotherium australe</i>	Int	YPM VPPU 15598	97.7	3.6	(1.4–9.0)	—	—	—	20.9	2.8	(1.4–5.6)	Sinclair (1909: pl. III, fig. 3)	
<i>Protypotherium praerutatum</i>	Int	YPM VPPU 15386	87.1	2.4	(1.0–6.2)	—	—	—	22.4	3.7	(1.9–7.2)	Sinclair (1909: pl. V, fig. 21)	

Species	Family	Specimen	CbL		HBL		OCW		Source(s)	
			M (mm)	BM	95% PI	M (cm)	BM	95% PI		
<i>Mesotherium cristatum</i>	Mes	MNHN PAM 2	275.7	94.0	(37.0–238.5)	-	-	60.7	105.5	(53.3–209.0) Fernández-Monescillo (2018: app. III, figs. 2–3)
<i>Mesotherium cristatum</i> ^f	Mes	(Reconstruction)	-	-	-	150.0	102.4	(52.2–201.1)	-	-
<i>Microtatherium choquecoense</i>	Mes	MNHN-BOL-V 11709	-	-	-	-	-	32.7	13.5	(6.8–26.7) Fernández-Monescillo (2018: app. III, figs. 2–3)
<i>Plesiorytherium achirense</i>	Mes	MNHN ACH 26	187.7	29.0	(11.5–73.6)	-	-	42.3	32.4	(16.4–64.0) Fernández-Monescillo (2018: fig. VII.3–4)
<i>Plesiorytherium achirense</i>	Mes	(Reconstruction)	191.1	30.7	(12.1–77.9)	110.0	40.7	(20.7–79.9)	-	-
<i>Plesiorytherium casiriense</i>	Mes	MNHN-BOL-V 239.0	61.0	(24.1–154.8)	-	-	-	54.7	75.2	(38.0–149.1) Cerdéñez et al. (2012: fig. 2)
<i>Plesiorytherium pulchrum</i>	Mes	AMNH 14509	-	-	-	-	-	50.5	58.0	(29.3–115.0) Fernández-Monescillo (2018: app. III, figs. 2–3)
<i>Plesiorytherium subinsigne</i>	Mes	MACN-Pv 8469	-	-	-	-	-	66.4	140.7	(71.1–279.1) Fernández-Monescillo (2018: app. III, figs. 2–3)
<i>Typhlotheriopsis chasticensis</i>	Mes	MLP 36-XII-10-2	223.8	49.9	(19.7–126.6)	-	-	56.8	84.9	(42.9–168.2) Fernández-Monescillo (2018: app. III, figs. 2–3)
<i>Archaeohipparion patagonicus</i>	Arc	MACN-A.52-617	142.8	13.4	(4.8–31.1)	-	-	29.5	10.0	(4.8–18.8) Bilete et al. (2009: table 4b)
<i>Archaeohipparion anguinivittatum</i>	Arc	SGOPV 2900	97.4	3.5	(1.4–8.9)	-	-	21.8	3.3	(1.7–6.5) Croft et al. (2003: fig. 11)
<i>Hegetotherium mirabile</i>	Heg	FMNH PM 13064	107.9	4.9	(2.0–12.5)	-	-	24.4	4.9	(2.5–9.7) Present study
<i>Hemiheterotherium trilobus</i>	Heg	(Composite)	130.8	9.3	(3.7–23.4)	-	-	30.2	10.4	(5.2–20.5) Croft and Anaya (2006: fig. 3)
<i>Pachyrukhos moyani</i>	Heg	AMNH 9129	70.2	1.2	(0.5–2.9)	-	-	16.6	1.2	(0.6–2.4) Present study
<i>Pachyrukhos moyani</i>	Heg	YPM VPPU 15743	75.9	1.5	(0.6–3.8)	-	-	19.0	2.0	(1.0–4.0) Sinclair (1909: pl. X)
<i>Pachyrukhos moyani</i> ^g	Heg	AMNH Composite	67.2	1.0	(0.4–2.5)	34.9	1.3	(0.7–2.6)	-	-
<i>Paedotherium bonaerense</i>	Heg	MACN-Pv 7253	75.4	1.5	(0.6–3.8)	-	-	16.2	1.1	(0.6–2.2) Ercoli et al. (2021a: fig. 3, 2021b, fig. 5)
<i>Paedotherium typicum</i>	Heg	AMNH 45914	70.9	1.2	(0.5–3.1)	-	-	14.1	0.7	(0.3–1.3) Present study
<i>Paedotherium typicum</i>	Heg	MMP 1008-M	79.9	1.8	(0.7–4.6)	42.7	2.4	(1.2–4.8)	2.1	(1.1–4.2) Ercoli pers. comm.
<i>Paedotherium typicum</i> ^h	Heg	PVL 3386	72.2	1.3	(0.5–3.2)	-	-	17.3	1.4	(0.7–2.8) Ercoli et al. (2021a: fig. 3, 2021b, figs. 5, 8)

Species	Family	Specimen	CbL	HBL			OCW			Source(s)
				M (mm)	BM	95% PI	M (cm)	BM	95% PI	
<i>Prosotherium garzoniⁱ</i>		Heg	AMNH 29574	101.0	4.0	(1.6–10.1)	39.6	2.0	(1.0–3.8)	— Simpson (1945: pl. 1), present study
<i>Tremacyllus intermedius^j</i>		Heg	MACN-Pv 2434	58.8	0.6	(0.2–1.6)	—	—	—	Ercoli et al. (2021a: fig. 3, 2021b: fig. 5)

^aComposite mount^bCarrillo and Asher (2017: fig. 3b) figure the occiput of MPEF-PV 8166 in occipital view. However, the scale on this image appears to be a lapsus, and original photos of the specimen suggest the occiput is at twice the scale figured in the study (Carrillo, pers. comm.)^cThe holotype of *Mendozatherium fierensis*, MCNAM-PV 4004, is a nearly complete skull 202 mm in length only missing the premaxillae. The total length of the skull was estimated by filling in the missing regions from MCNAM-PV 3846, which preserves this region^dCBL estimated by placing images of mandible, basicranial fragment, and rostrum back in articulation^eThis is a mounted replica (or at least mostly replica) skeleton of *Miocachilius anomopodus* in the collections of the AMNH. The specimen does not have a collection number and there is no reliable data on where it came from (A. Gishlick, pers. comm.). It may be a cast of UCMP material (possibly UCMP 30944?)^fValue from caption^gBased on AMNH 9242, 9481, and 9283 (Sinclair 1909)^hHBL is calculated by taking length of C1–7, 12 thoracolumbars, and sacrum and estimating missing pieces based on specimens figured in Scott (1990) and Ercoli et al. (2021a)ⁱFollows taxonomy of Soane et al. (2017)^jFollows taxonomy of Cerdeño and Bond (1998)

Supplementary Information The online version contains supplementary material available at <https://doi.org/10.1007/s10914-023-09669-1>.

Acknowledgements We thank M. Ercoli and D. García-López for help in obtaining data for *Paedotherium*; J. Galkin and J. Meng (AMNH) and A. F. Vanegas and R. D. Vanegas (MHNT) for providing photographs and measurements of specimens in their care; and C. Suarez for helping facilitate contact with the MHNT during the COVID-19 pandemic. In addition, we thank A. Elissamburu and A. Hubbe, whose comments and insights improved this manuscript, and F. Pujos, who managed the editorial process as Associate Editor. We gratefully acknowledge the following colleagues who generously provided data and advice that contributed to our database of extant mammal head-body length and body mass: O. Aleuy (*Ovis dalli*); A. Bertassoni (*Myrmecophaga tridactyla*); C. Curry, D. Smith, E. Stahler, and M. Watson (*Canis lupus*, YELL); B. Coyner (OMNH); M. Ercoli (*Lynodon patagonicus*); A. Feijó (*Dasyurus* spp.); E. Gonzalez (MNHN, Caviomorpha); A. Hornsby (UMZM); S. Ingelby (AM, Marsupialia); Lim and Seymour (ROM *Loxodonta*); L. Lessa (*Euryzygomatomys*); P. Kamminga (ZMA.MAM, *Bubalis quarelesi*); V. Mathis (UF); F. Nascimento (*Leopardus*); R. Ojala-Barbour and J. Brito (*Caenolestes*); J. Pérez-Flores (*Tapirus* spp.); R. Rose (Australian mammals); P. Sadler and G. Shannon (*Hippopotamus amphibius*); R. Voss (AMNH, Didelphidae); and M. Xavier, P. Gonçalves, and F. Khaled (*Chrysocyon brachyurus*, NPM). Additionally, we express a general debt of gratitude towards all field collectors whose fieldwork yielded the thousands of specimens on which our comparative database is based.

Author contributions DAC and AN conceived of the project; AN and RKE collected and analyzed the data; DAC and RKE wrote the initial draft of the manuscript; AN and RKE drafted the illustrations; all authors read, revised, and approved the final version the manuscript and its associated supplementary files.

Availability of data and material All data generated or analyzed during this study are included in this published article and its supplementary information files.

Declarations

Competing interests DAC is editor-in-chief of the Journal of Mammalian Evolution but was not involved in the review or evaluation process for this manuscript.

References

- Alexander RM (1980). Forces in animal joints. Eng Med 9:93–97. https://doi.org/10.1243/EMED_JOUR_1980_009_022_02
- Alexander RM (1985) Body size and limb design in primates and other mammals. In: Jungers WL (ed) Size and Scaling in Primate Biology. Springer, New York, pp 337–343
- Anderson JF, Hall-Martin A, Russell DA (1985) Long-bone circumference and weight in mammals, birds and dinosaurs. J Zool (Lond) 207:53–61. <https://doi.org/10.1111/j.1469-7998.1985.tb04915.x>
- Ane C (2021) Re: [R-sig-phylo] Model selection and PGLS. R-sig-phylo mailing list. <https://www.mail-archive.com/r-sig-phylo@r-project.org/msg05774.html>. Accessed June 29, 2021.
- Ansell, WFH (1956) Standardization of field data on mammals. Zool Africana 1:97–113. <https://doi.org/10.1080/00445096.1965.11447303>
- Anyonge W (1993) Body mass in large extant and extinct carnivores. J Zool (Lond) 231:339–350. <https://doi.org/10.1111/j.1469-7998.1993.tb01922.x>

- Armella MA (2019) Sistemática, bioestratigrafía y paleobiogeografía de los notoungulados del Neógeno del Noroeste Argentino. Dissertation, Universidad Nacional de Tucumán
- Asher RJ, Lin KH, Kardjilov N, Hautier L (2011) Variability and constraint in the mammalian vertebral column. *J Evol Biol* 24:1080–1090. <https://doi.org/10.1111/j.1420-9101.2011.02240.x>
- Auguie B (2017) gridExtra: Miscellaneous Functions for "Grid" Graphics, R package version 2.3. R Foundation for Statistical Computing, Vienna, Austria. <https://CRAN.R-project.org/package=gridExtra>. Accessed August 14, 2022.
- Bartholomew GA (1981) A matter of size: an examination of endothermy in insects and terrestrial vertebrates. In: Heinrich B (ed) Insect Thermoregulation. Wiley, New York, pp 45–78
- Basu C, Falkingham PL, Hutchinson JR (2016) The extinct, giant giraffid *Sivatherium giganteum*: skeletal reconstruction and body mass estimation. *Biol Lett* 12:20150940. <https://doi.org/10.1098/rsbl.2015.0940>
- Bates KT, Falkingham PL, Macaulay S, Brassey C, Maidment SCR (2015) Downsizing a giant: re-evaluating *Dreadnoughtus* body mass. *Biol Lett* 11:20150215. <https://doi.org/10.1098/rsbl.2015.0215>
- Baty F, Ritz C, Charles S, Brutsche M, Flandrois J-P, Delignette-Muller M-L (2015) A Toolbox for Nonlinear Regression in R: The Package nlstools. *J Stat Softw* 1(5). <https://doi.org/10.18637/jss.v066.i05>
- Berqvist L, Metello TM (2011) The first postcranial bones of *Notostylops* Simpson, 1948, from Chubut, Argentina (Barrancan). *Ameghiniana* 48:143R
- Billet G (2011) Phylogeny of the Notoungulata (Mammalia) based on cranial and dental characters. *J Syst Palaeontol* 9:481–497. <https://doi.org/10.1080/14772019.2010.528456>
- Billet G, Patterson B, Muizon C de (2009) Craniodental anatomy of late Oligocene archaeohyracids (Notoungulata, Mammalia) from Bolivia and Argentina and new phylogenetic hypotheses. *Zool J Linn Soc* 155:458–509. <https://doi.org/10.1111/j.1096-3642.2008.00445.x>
- Bocchino de Ringuelet A (1957) Estudio del género *Chasicotherium* Cabrera y Kraglievich 1931 (Notoungulata - Homalodotheriidae). *Ameghiniana* 1:7–14
- Bond M (1999) Quaternary native ungulates of southern South America. A synthesis. In: Rabassa J, Salemme M (eds) Quaternary of South America and Antarctic Peninsula. A.A. Balkema, Rotterdam, pp 177–205
- Brassey CA (2016) Body-mass estimation in paleontology: A review of volumetric techniques. *Paleontol Soc Pap* 22:133–156. <https://doi.org/10.1017/scs.2017.12>
- Brassey CA, Maidment SCR, Barrett PM (2015) Body mass estimates of an exceptionally complete *Stegosaurus* (Ornithischia: Thyreophora): comparing volumetric and linear bivariate mass estimation methods. *Biol Lett* 11:20140984
- Brassey CA, O'Mahoney TG, Chamberlain AT, Sellers WI (2018) A volumetric technique for fossil body mass estimation applied to *Australopithecus afarensis*. *J Human Evol* 115:47–64. <https://doi.org/10.1016/j.jhevol.2017.07.014>
- Buckley M (2015) Ancient collagen reveals evolutionary history of the endemic South American 'ungulates'. *Proc R Soc B* 282:20142671
- Cabrera A, Kraglievich L (1931) Diagnosis previas de los ungulados fósiles del Arroyo Chasicó. *Notas Prelim Mus La Plata* 1:107–113
- Campione NE (2017) Extrapolating body masses in large terrestrial vertebrates. *Paleobiology* 43:693–699. <https://doi.org/10.1017/pab.2017.9>
- Campione NE, Evans DC (2012) A universal scaling relationship between body mass and proximal limb bone dimensions in quadrupedal terrestrial tetrapods. *BMC Biol* 10:60. <https://doi.org/10.1186/1741-7007-10-60>
- Campione NE, Evans DC (2020) The accuracy and precision of body mass estimation in non-avian dinosaurs. *Biol Rev (Camb)* 95:1759–1797. <https://doi.org/10.1111/brv.12638>
- Campione NE, Evans DC, Brown CM and Carrano MT (2014) Body mass estimation in non-avian bipeds using a theoretical conversion to quadruped stylopodial proportions. *Methods Ecol Evol* 5(9):913–923. <https://doi.org/10.1111/2041-210X.12226>
- Cardonatto MC, Melchor RN (2018) Large mammal burrows in late Miocene calcic paleosols from central Argentina: paleoenvironment, taphonomy and producers. *PeerJ* 6:e4787. <https://doi.org/10.7717/peerj.4787>
- Carrillo JD, Asher RJ (2017) An exceptionally well-preserved skeleton of *Thomashuxleya externa* (Mammalia, Notoungulata), from the Eocene of Patagonia, Argentina. *Palaeontol Electron* 20:1–33
- Cassini GH, Cerdeño E, Villafañe AL, Muñoz NA (2012a) Paleobiology of Santacrucian native ungulates (Meridiungulata; Astrapotheria, Litopterna and Notoungulata). In: Vizcaíno SF, Kay RF, Bargo MS (eds) Early Miocene Paleobiology in Patagonia: High-Latitude Paleocommunities of the Santa Cruz Formation. Cambridge University Press, Cambridge, pp 243–286
- Cassini GH, Hernández Del Pino S, Muñoz NA, Acosta MVWG, Fernández M, Bargo MS, Vizcaíno SF (2017) Teeth complexity, hypsodonty and body mass in Santacrucian (early Miocene) notoungulates (Mammalia). *Earth Environ Sci Trans R Soc Edinb* 106:303–313. <https://doi.org/10.1017/S1755691016000153>
- Cassini GH, Mendoza M, Vizcaíno SF, Bargo MS (2011) Inferring habitat and feeding behaviour of early Miocene notoungulates from Patagonia. *Lethaia* 44:153–165. <https://doi.org/10.1111/j.1502-3931.2010.00231.x>
- Cassini GH, Vizcaíno SF (2012) An approach to the biomechanics of the masticatory apparatus of early Miocene (Santacrucian Age) South American ungulates (Astrapotheria, Litopterna, and Notoungulata): moment arm estimation based on 3D landmarks. *J Mamm Evol* 19:9–25. <https://doi.org/10.1007/s10914-011-9179-5>
- Cassini GH, Vizcaíno SF, Bargo MS (2012b) Body mass estimation in early Miocene native South American ungulates: a predictive equation based on 3D landmarks. *J Zool (Lond)* 287:53–64. <https://doi.org/10.1111/j.1469-7998.2011.00886.x>
- Catena AM, Croft DA (2020) What are the best modern analogs for ancient South American mammal communities? Evidence from ecological diversity analysis (EDA). *Palaeontol Electron* 23:a03. <https://doi.org/10.26879/962>
- Cerdeño E (2019) Updated synthesis of South American Mesotheriidae (Notoungulata) with emphasis on west-central Argentina. *Rev Paleobiol* 37:421–431
- Cerdeño E, Bond M (1998) Taxonomic revision and phylogeny of *Pae-dotherium* and *Tremacyllus* (Pachyrhynchinae, Hegetotheriidae, Notoungulata) from the late Miocene to Pleistocene of Argentina. *J Vertebr Paleontol* 18:799–811
- Cerdeño E, Contreras VH (2000) El esqueleto postcraneal de *Hemiheterotherium* (Hegetotheriidae, Notoungulata) del Mioceno superior de Puchuzum, San Juan, Argentina. *Rev Esp Paleontol* 15:171–179
- Cerdeño E, Vera B (2010) *Mendozahippus fierensis* gen. et sp. nov., new Notohippidae (Notoungulata) from the late Oligocene of Mendoza (Argentina). *J Vertebr Paleontol* 30:1805–1817. <https://doi.org/10.1080/02724634.2010.520781>
- Cerdeño E, Vera B (2015) A new Leontiniidae (Notoungulata) from the Late Oligocene beds of Mendoza Province, Argentina. *J Syst Palaeontol* 13:943–962. <https://doi.org/10.1080/14772019.2014.982727>
- Cerdeño E, Vera B, Schmidt GI, Pujos F, Quispe BM (2012) An almost complete skeleton of a new Mesotheriidae (Notoungulata) from the Late Miocene of Casira, Bolivia. *J Syst Palaeontol* 10:341–360. <https://doi.org/10.1080/14772019.2011.569576>
- Chaffee RG (1952) The Deseadan vertebrate fauna of the Scarratt Pocket, Patagonia. *Bull Am Mus Nat Hist* 98:509–562
- Christiansen P (1999) Scaling of the limb long bones to body mass in terrestrial mammals. *J Morphol* 239:167–190. [https://doi.org/10.1002/\(SICI\)1097-4687\(199902\)239:2%3C167::AID-JMOR5%3E3.0.CO;2-8](https://doi.org/10.1002/(SICI)1097-4687(199902)239:2%3C167::AID-JMOR5%3E3.0.CO;2-8)

- Cifelli RL (1993) The phylogeny of the native South American ungulates. In: Szalay FS, Novacek MJ, McKenna MC (eds) *Mammal Phylogeny: Placentals*. Springer-Verlag, New York, pp 195–216
- Coombs MC (1983) Large mammalian clawed herbivores: a comparative study. *Trans Am Philos Soc* 73:1–96
- Couto-Ribeiro G (2015) *Osteologia de Taubatherium paulacoutoi* Soria & Alvarenga, 1989 (Notoungulata, Leontiniidae) e de um novo Pyrotheria: dois mamíferos da Formação Tremembé, Brasil (SALMA Deseadense - Oligoceno Superior). Dissertation, Universidade de São Paulo
- Croft DA (1999) Placentalts: South American ungulates. In: Singer R (ed) *Encyclopædia of Paleontology*. Fitzroy-Dearborn Publishers, Chicago, Illinois, pp 890–906
- Croft DA (2000) Archaeohyracidae (Mammalia, Notoungulata) from the Tinguiririca Fauna, central Chile, and the evolution and paleoecology of South American mammalian herbivores. Dissertation, The University of Chicago
- Croft DA (2016) Horned Armadillos and Rafting Monkeys: The Fascinating Fossil Mammals of South America. Indiana University Press, Bloomington, Indiana
- Croft DA, Anaya F (2006) A new middle Miocene hegetotheriid (Notoungulata: Typotheria) and a phylogeny of the Hegetotheriidae. *J Vertebr Paleontol* 26:387–399
- Croft DA, Anderson LC (2008) Locomotion in the extinct notoungulate *Protypotherium*. *Palaeontol Electron* 11.1.1A:1–20
- Croft DA, Lorente M (2021) No evidence for parallel evolution of cursorial limb adaptations among Neogene South American native ungulates (SANUs). *PLoS ONE* 16:e0256371. <https://doi.org/10.1371/journal.pone.0256371>
- Croft DA, Weinstein D (2008) The first application of the mesowear method to endemic South American ungulates (Notoungulata). *Palaeogeogr Palaeoclimatol Palaeoecol* 269:103–114. <https://doi.org/10.1016/j.palaeo.2008.08.007>
- Croft DA, Bond M, Flynn JJ, Reguero MA, Wyss AR (2003) Large archaeohyracids (Typotheria, Notoungulata) from central Chile and Patagonia including a revision of Archaeotypotherium. *Fieldiana Geol (NS)* 49:1–38
- Croft DA, Flynn JJ, Wyss AR (2004) Notoungulata and Litopterna of the early Miocene Chucal Fauna, northern Chile. *Fieldiana Geol (NS)* 50:1–52
- Croft DA, Flynn JJ, Wyss AR (2008) The Tinguiririca Fauna of Chile and the early stages of "modernization" of South American mammal faunas. *Arq Mus Nac (Rio J)* 66:191–211
- Croft DA, Gelfo JN, López GM (2020) Splendid innovation: The South American native ungulates. *Annu Rev Earth Planet Sci* 48:249–290. <https://doi.org/10.1146/annurev-earth-072619-060126>
- Damuth J (1990) Problems in estimating body masses of archaic ungulates using dental measurements. In: Damuth J, MacFadden BJ (eds) *Body Size in Mammalian Paleobiology: Estimation and Biological Implications*. Cambridge University Press, Cambridge, United Kingdom, pp 229–253
- Damuth J, MacFadden BJ (eds) (1990) *Body Size in Mammalian Paleobiology: Estimation and Biological Implications*. Cambridge University Press, Cambridge, United Kingdom
- Del Pino SH (2018) Anatomía y sistemática de los Toxodontidae (Notoungulata) de la Formación Santa Cruz, Mioceno temprano, Argentina. Dissertation, Universidad Nacional de La Plata
- Dunn RE, Strömberg CAE, Madden RH, Kohn MJ, Carlini AA (2015) Linked canopy, climate, and faunal change in the Cenozoic of Patagonia. *Science* 347:258–261. <https://doi.org/10.1126/science.1260947>
- Egi N (2001) Body mass estimates in extinct mammals from limb bone dimensions: the case of North American hyaenodontids. *Paleontol* 44:497–528. <https://doi.org/10.1111/1475-4983.00189>
- Eisenberg JF (1990) The behavioral/ecological significance of body size in the Mammalia. In: Damuth J, MacFadden BJ (eds) *Body Size in Mammalian Paleobiology: Estimation and Biological Implications*. Cambridge University Press, Cambridge, United Kingdom, pp 25–37
- Elbroch M (2006) *Animal Skulls. A Guide to North American Species*. Stackpole Books, Mechanicsburg, Pennsylvania
- Elissamburu A (2004) Análisis morfométrico y morfológico del esqueleto appendicular de *Paedotherium* (Mammalia, Notoungulata). *Ameghiniana* 41:363–380
- Elissamburu A (2010) Estudio biomecánico y morfológico del esqueleto apendicular de *Homalodotherium* Flower 1873 (Mammalia, Notoungulata). *Ameghiniana* 47:25–43
- Elissamburu A (2012) Estimación de la masa corporal en géneros del Orden Notoungulata. *Estud Geol (Madr)* 68:91–111
- Elissamburu A, Vizcaíno SF (2005) Diferenciación morfométrica del húmero y fémur de las especies de *Paedotherium* (Mammalia, Notoungulata) del Plioceno y Pleistoceno temprano. *Ameghiniana* 42:159–166
- Engelman RK (2022) Occipital condyle width (OCW) is a highly accurate predictor of body mass in therian mammals. *BMC Biol* 20:37. <https://doi.org/10.1186/s12915-021-01224-9>
- Ercoli MD, Álvarez A, Candela AM (2019) Sciromorphy outside rodents reveals an ecomorphological convergence between squirrels and extinct South American ungulates. *Common Biol* 2:202. <https://doi.org/10.1038/s42003-019-0423-5>
- Ercoli MD, Álvarez A, Moyano SR, Youlatos D, Candela AM (2021a) Tracing the paleobiology of *Paedotherium* and *Tremacyllus* (Pachyrhukhinae, Notoungulata), the latest sciromorph South American native ungulates - Part I: Snout and masticatory apparatus. *J Mamm Evol* 28:377–409. <https://doi.org/10.1007/s10914-020-09516-7>
- Ercoli MD, Álvarez A, Youlatos D, Moyano SR, Candela AM (2021b) Tracing the paleobiology of *Paedotherium* and *Tremacyllus* (Pachyrhukhinae, Notoungulata), the latest sciromorph South American native ungulates - Part II: Orbital, auditory, and occipitocervical regions. *J Mamm Evol* 28:411–433. <https://doi.org/10.1007/s10914-020-09518-5>
- Fariña RA, Alvarez F (1994) La postura de *Toxodon*: un nueva reconstrucción. *Acta Geol Leopold* 17:565–571
- Fariña RA, Vizcaíno SF, Bargo MS (1998) Body mass estimations in Lujanian (late Pleistocene - early Holocene of South America) mammal megafauna. *Mastozool Neotrop* 5:87–108
- Fernández-Monescillo M, Quispe BM, Pujos F, Antoine P-O (2018) Functional anatomy of the forelimb of *Plesiotypotherium achirense* (Mammalia, Notoungulata, Mesotheriidae) and evolutionary insights at the family level. *J Mamm Evol* 25:197–211. <https://doi.org/10.1007/s10914-016-9372-7>
- Fernández-Monescillo M, Antoine P-O, Pujos F, Gomes Rodrigues H, Mamani Quispe B, Orliac M (2019) Virtual endocast morphology of Mesotheriidae (Mammalia, Notoungulata, Typotheria): New insights and implications on notoungulate encephalization and brain evolution. *J Mamm Evol* 26:85–100. <https://doi.org/10.1007/s10914-017-9416-7>
- Fernández-Monescillo M, Croft DA, Pujos F, Antoine P-O (2022) Resolution of the long-standing controversy over the type species of the genus *Pseudotypotherium* (Mesotheriidae, Notoungulata). *Palaeoworld*. <https://doi.org/10.1016/j.palwor.2022.09.009>
- Ferrero BS, Schmidt GI, Pérez-García MI, Perea D, Ribeiro AM (2022) A new Toxodontidae (Mammalia, Notoungulata) from the upper Pliocene–lower Pleistocene of Uruguay. *J Vertebr Paleontol* 41:e2023167. <https://doi.org/10.1080/02724634.2021.2023167>
- Forasiepi AM, Cerdeño E, Bond M, Schmidt G, Naipauer M, Straehl FR, Martinelli AG, Garrido AC, Schmitz MD, Crowley JL (2015) New toxodontid (Notoungulata) from the Early Miocene of Mendoza, Argentina. *Paläontol Z* 89:611–634. <https://doi.org/10.1007/s12542-014-0233-5>
- Garland T, Jr., Ives AR (2000) Using the past to predict the present: Confidence intervals for regression equations in phylogenetic

- comparative methods. Am Nat 155:346–364. <https://doi.org/10.1086/303327>
- Geist V (1998) Deer of the World: Their Evolution, Behaviour, and Ecology. Stackpole Books, Mechanicsburg, PA
- Giannini NP, García-López DA (2014) Ecomorphology of mammalian fossil lineages: identifying morphotypes in a case study of endemic South American ungulates. J Mamm Evol 21:195–212. <https://doi.org/10.1007/s10914-013-9233-6>
- Gomes Rodrigues H, Herrel A, Billet G (2017) Ontogenetic and life history trait changes associated with convergent ecological specializations in extinct ungulate mammals. Proc Natl Acad Sci U S A 114:1069–1074. <https://doi.org/10.1073/pnas.1614029114>
- Guérin C, Faure M (2013) Un nouveau Toxodontidae (Mammalia, Notoungulata) du Pléistocène supérieur du Nordeste du Brésil. Geodiversitas 35:155–205
- Gunga HC, Suthau T, Bellmann A, Stoinski S, Friedrich A, Trippel T, Kirsch K, Hellwich O (2008) A new body mass estimation of *Brachiosaurus brancai* Janensch, 1914 mounted and exhibited at the Museum of Natural History (Berlin, Germany). Foss Rec 11:33–38. <https://doi.org/10.1002/mmng.200700011>
- Hallgrímsson B, Maiorana V (2000) Variability and size in mammals and birds. Biol J Linn Soc 70:571–595. <https://doi.org/10.1111/j.1095-8312.2000.tb00218.x>
- Hart LJ, Campione NE, McCurry MR (2022) On the estimation of body mass in temnospondyls: a case study using the large-bodied *Eryops* and *Paracyclotosaurus*. Palaeontology 65:e12629. <https://doi.org/10.1111/pala.12629>
- Hitz RB, Reguero M, Wyss AR, Flynn JJ (2000) New interatheriines (Interatheriidae, Notoungulata) from the Paleogene of central Chile and southern Argentina. Fieldiana Geol (NS) 42:1–26
- Hopkins SSB (2018) Estimation of body size in fossil mammals. In: Croft DA, Su DF, Simpson SW (eds) Methods in Paleoecology: Reconstructing Cenozoic Terrestrial Environments and Ecological Communities. Springer Nature, Cham, Switzerland, pp 7–22
- Horikoshi M, Tang Y (2016) ggfortify: Data Visualization Tools for Statistical Analysis Results., R package version 0.4.15. R Foundation for Statistical Computing, Vienna, Austria. <https://CRAN.R-project.org/package=ggfortify>. Accessed November 13, 2022.
- Janis CM (1990) Correlation of cranial and dental variables with body size in ungulates and macropodids. In: Damuth J, MacFadden BJ (eds) Body Size in Mammalian Paleobiology: Estimation and Biological Implications. Cambridge University Press, Cambridge, pp 255–300
- Jungers WL (1990) Problems and methods in reconstructing body size in fossil primates. In: Damuth J, MacFadden BJ (eds) Body Size in Mammalian Paleobiology: Estimation and Biological Implications. Cambridge University Press, Cambridge, pp 103–118
- Kay RF, Madden RH (1997) Paleogeography and paleoecology. In: Kay RF, Madden RH, Cifelli RL, Flynn JJ (eds) Vertebrate Paleontology in the Neotropics: The Miocene Fauna of La Venta, Colombia. Smithsonian Institution Press, Washington, D.C., pp 520–550
- Khan MKbM (1997) Status and action plan of the Malayan tapir (*Tapirus indicus*). In: Brooks DM, Bodmer RE, Matola S (eds) Tapirs - Status Survey and Conservation Action Plan. IUCN, Cambridge, pp 23–28
- Kilbourne BM, Hoffman LC (2013) Scale effects between body size and limb design in quadrupedal mammals. PloS ONE 8:e78392. <https://doi.org/10.1371/journal.pone.0078392>
- Kramarz AG (2002) Roedores chinchilloideos (Hystricognathi) de la Formación Pinturas, Mioceno temprano-medio de la provincia de Santa Cruz, Argentina. Rev Mus Argent Cien Nat 4:167–180
- Li Y, Brinkworth A, Green E, Oyston J, Wills M, Ruta M (2023) Divergent vertebral formulae shape the evolution of axial complexity in mammals. Nat Ecol Evol 7:367–381. <https://doi.org/10.1038/s41559-023-01982-5>
- Loomis FB (1914) The Deseado Formation of Patagonia. Runford Press, Concord, New Hampshire
- Lorente M, Gelfo JN, López GM (2019) First skeleton of the notoungulate mammal *Notostylops murinus* and palaeobiology of Eocene Notostylopidae. Lethaia 52:244–259. <https://doi.org/10.1111/let.12310>
- MacFadden BJ (2005) Diet and habitat of toxodont megaherbivores (Mammalia, Notoungulata) from the late Quaternary of South and Central America. Quat Res 64:113–124
- MacPhee RDE (2014) The *serialis* bone, interparietals, "X" elements, entotympanics, and the composition of the notoungulate caudal cranium. Bull Am Mus Nat Hist 384:1–69. <https://doi.org/10.1206/384.1>
- Madden RH (1990) Miocene Toxodontidae (Notoungulata, Mammalia) from Colombia, Ecuador, and Chile. Dissertation, Duke University
- Madden RH (2015) Hypsodonty in Mammals. Cambridge University Press, Cambridge
- Marshall LG, Cifelli RL (1990) Analysis of changing diversity patterns in Cenozoic land mammal age faunas, South America. Palaeovertebrata 19:169–210
- Marshall LG, Hoffstetter R, Pascual R (1983) Mammals and stratigraphy: geochronology of the mammal-bearing Tertiary of South America. Palaeovertebrata Mém Extraordin 1983:1–93
- Martínez G, Dozo MT, Gelfo JN, Marani H (2016) Cranial morphology of the late Oligocene Patagonian notohippid *Rhynchippus equinus* Ameghino, 1897 (Mammalia, Notoungulata) with emphases in basicranial and auditory region. PLoS ONE 11:e0156558. <https://doi.org/10.1371/journal.pone.0156558>
- McGrath AJ, Anaya F, Croft DA (2018) Two new macraucheniiids (Mammalia: Litopterna) from the late middle Miocene (Laventan South American Land Mammal Age) of Quebrada Honda, Bolivia. J Vertebr Paleontol 38:e1461632. <https://doi.org/10.1080/02724634.2018.1461632>
- Mendoza M, Janis CM, Palmqvist P (2006) Estimating the body mass of extinct ungulates: a study on the use of multiple regression. J Zool (Lond) 270:90–101. Doi <https://doi.org/10.1111/J.1469-7998.2006.00094.X>
- Narita Y, Kuratani S (2005) Evolution of the vertebral formulae in mammals: A perspective on developmental constraints. J Exp Zool Part B Mol Dev Evol 304B:91–106. Doi <https://doi.org/10.1002/jez.B.21029>
- Naughton D (2012) The Natural History of Canadian Mammals. University of Toronto Press, Toronto
- Owen R (1838) Fossil Mammalia (No. I of Part I). In: Darwin CR (ed) The Zoology of the Voyage of H.M.S. Beagle. Smith Elder and Co, London, pp 1–40
- Palazzi L, Barreda V (2012) Fossil pollen records reveal a late rise of open-habitat ecosystems in Patagonia. Nat Commun 3:1294. <https://doi.org/10.1038/ncomms2299>
- Paradis E, Schliep K (2018) ape 5.0: an environment for modern phylogenetics and evolutionary analyses in R. Bioinformatics 35:526–528
- Pascual R, Ortiz-Jaureguizar E, Prado JL (1996) Land mammals: paradigm for Cenozoic South American geobiotic evolution. In: Arratia G (ed) Contributions of Southern South America to Vertebrate Paleontology. München Geowiss Abh 30 (A), Munich, pp 265–319
- Patterson B, Pascual R (1968) The fossil mammal fauna of South America. Q Rev Biol 43:409–451
- Perini FA, Macrini TE, Flynn JJ, Bamba K, Ni X, Croft DA, Wyss AR (2022) Comparative endocranial anatomy, encephalization, and phylogeny of Notoungulata (Placentalia, Mammalia). J Mamm Evol 29:369–394. <https://doi.org/10.1007/s10914-021-09583-4>

- Pinheiro J, Bates D, DebRoy S, Sarkar D, Team RC (2019) nlme: Linear and Nonlinear Mixed Effects Models. <https://CRAN.R-project.org/package=nlme>. Accessed October 10, 2022.
- Price SA, Hopkins SSB (2015) The macroevolutionary relationship between diet and body mass across mammals. *Biol J Linn Soc* 115:173–184. <https://doi.org/10.1111/bij.12495>
- Prothero JW (1992) Scaling of bodily proportions in adult terrestrial mammals. *Am J Physiol* 262:R492–503. <https://doi.org/10.1152/ajpregu.1992.262.3.R492>
- R Core Team (2021) R: A Language and Environment for Statistical Computing. R Foundation for Statistical Computing, Vienna, Austria. <http://www.R-project.org/>
- Reguero MA, Prevosti FJ (2010) Rodent-like notoungulates (Typotheria) from Gran Barranca, Chubut Province, Argentina: phylogeny and systematics. In: Madden RH, Carlini AA, Vucetich MG, Kay RF (eds) The Paleontology of Gran Barranca. Evolution and Environmental Change through the Middle Cenozoic of Patagonia. Cambridge University Press, Cambridge, pp 152–169
- Reguero MA, Candela AM, Cassini GH (2010) Hypodonty and body size in rodent-like notoungulates. In: Madden RH, Carlini AA, Vucetich MG, Kay RF (eds) The Paleontology of Gran Barranca. Evolution and Environmental Change through the Middle Cenozoic of Patagonia. Cambridge University Press, Cambridge, pp 362–371
- Riggs ES (1937) Mounted skeleton of *Homalodotherium*. *Geol Ser, Field Mus Nat Hist* 6:233–243
- Rinderknecht A, Blanco RE (2008) The largest fossil rodent. *Proc R Soc B* 275:923–928. <https://doi.org/10.1098/rspb.2007.1645>
- Robinson D, Hayes A, Couch S (2022) broom: Convert Statistical Objects into Tidy Tibbles, R package version 1.0.1. R Foundation for Statistical Computing, Vienna, Austria. <https://CRAN.R-project.org/package=broom>. Accessed October 9 2022.
- Romano M, Manucci F, Palombo MR (2021) The smallest of the largest: new volumetric body mass estimate and in-vivo restoration of the dwarf elephant *Palaeoloxodon* ex gr. *P. falconeri* from Spinagallo Cave (Sicily). *Hist Biol* 33:340–353. <https://doi.org/10.1080/08912963.2019.1617289>
- Roth VL (1990) Insular dwarf elephants; a case study in body mass estimation and ecological inference. In: Damuth J, MacFadden BJ (eds) Body Size in Mammalian Paleobiology: Estimation and Biological Implications. Cambridge University Press, Cambridge, United Kingdom, pp 151–179
- Rovereto C (1914) Los estratos araucanos y sus fósiles. *An Mus Nac Hist Nat Buenos Aires* 25:1–247
- Rovinsky DS, Evans AR, Martin DG, Adams JW (2020) Did the thylacine violate the costs of carnivory? Body mass and sexual dimorphism of an iconic Australian marsupial. *Proc R Soc B* 287:20201537. <https://doi.org/10.1098/rspb.2020.1537>
- Ruff C (1990) Body mass and hindlimb bone cross-sectional and articular dimensions in anthropoid primates. In: Damuth J, MacFadden BJ (eds) Body Size in Mammalian Paleobiology: Estimation and Biological Implications. Cambridge University Press, Cambridge, United Kingdom, pp 119–149
- Ruff CB (2003) Long bone articular and diaphyseal structure in Old World monkeys and apes. II: Estimation of body mass. *Am J Phys Anthropol* 120:16–37. <https://doi.org/10.1002/ajpa.10118>
- Sánchez-Villagra MR, Aguilera O, Horowitz I (2003) The anatomy of the world's largest extinct rodent. *Science* 301:1708–1710
- Sánchez-Villagra MR, Narita Y, Kuratani S (2007) Thoracolumbar vertebral number: The first skeletal synapomorphy for afroterian mammals. *Syst Biodivers* 5:1–7. <https://doi.org/10.1017/S147720006002258>
- Scarano AC, Carlini AA, Illius AW (2011) Interatheriidae (Typotheria; Notoungulata), body size and paleoecology characterization. *Mamm Biol* 76:109–114
- Schmidt-Nielsen K (1984) Scaling: Why is Animal Size so Important? Cambridge University Press, Cambridge
- Schneider CA, Rasband WS, Eliceiri KW (2012) NIH Image to ImageJ: 25 years of image analysis. *Nat Methods* 9:671–675. <https://doi.org/10.1038/nmeth.2089>
- Schultz AH (1929) The technique of measuring the outer body of human fetuses and of primates in general. *Contrib Embryol* 117:213–257.
- Scott WB (1910) Mammalia of the Santa Cruz Beds. Volume VII, Paleontology. Part I, Litopterna. In: Scott WB (ed) Reports of the Princeton University Expeditions to Patagonia, 1896–1899. Princeton University, E. Schweizerbart'sche Verlagshandlung (E. Nägele), Stuttgart, pp 1–156
- Scott WB (1912) Mammalia of the Santa Cruz Beds. Volume VI, Paleontology. Part II, Toxodonta. In: Scott WB (ed) Reports of the Princeton University Expeditions to Patagonia, 1896–1899. Princeton University, E. Schweizerbart'sche Verlagshandlung (E. Nägele), Stuttgart, pp 111–238
- Scott WB (1930) A partial skeleton of *Homalodontotherium* from the Santa Cruz beds of Patagonia. *Mem Field Mus Nat Hist* 50:1–34
- Scott WB (1937) A History of Land Mammals in the Western Hemisphere, Second Ed. MacMillan Co., New York
- Scott KM (1985) Allometric trends and locomotor adaptations in the Bovidae. *Bull Am Mus Nat Hist* 179:199–288
- Scott KM (1990) Postcranial dimensions of ungulates as predictors of body mass. In: Damuth J, MacFadden BJ (eds) Body Size in Mammalian Paleobiology: Estimation and Biological Implications. Cambridge University Press, Cambridge, pp 301–335.
- Seckel L, Janis C (2008) Convergences in scapula morphology among small cursorial mammals: an osteological correlate for locomotor specialization. *J Mamm Evol* 15:261–279. Doi <https://doi.org/10.1007/S10914-008-9085-7>
- Sellers WI, Hepworth-Bell J, Falkingham PL, Bates KT, Brassey CA, Egerton VM, Manning PL (2012) Minimum convex hull mass estimations of complete mounted skeletons. *Biol Lett* 8:842–845. <https://doi.org/10.1098/rsbl.2012.0263>
- Seoane FD, Roig Juñent S, Cerdeño E (2017) Phylogeny and paleobiogeography of Hegetotheriidae (Mammalia, Notoungulata). *J Vertebr Paleontol* 37:e1278547. <https://doi.org/10.1080/02724634.2017.1278547>
- Shockley BJ (1997) Two new notoungulates (Family Notohippidae) from the Salla Beds of Bolivia (Deseadan: late Oligocene): systematics and functional morphology. *J Vertebr Paleontol* 17:584–599
- Shockley BJ, Anaya F (2008) Postcranial osteology of mammals from Salla, Bolivia (late Oligocene): form, function, and phylogenetic implications. In: Sargis EJ, Dagosto M (eds) Mammalian Evolutionary Morphology: A Tribute to Frederick S. Szalay. Springer, New York, pp 135–157
- Shockley BJ, Flynn JJ (2007) Morphological diversity in the postcranial skeleton of Casamayoran (?middle to late Eocene) Notoungulata and foot posture in notoungulates. *Am Mus Novit* 3601:1–26. [https://doi.org/10.1206/0003-0082\(2007\)3601\[1:MDITPS\]2.0.CO;2](https://doi.org/10.1206/0003-0082(2007)3601[1:MDITPS]2.0.CO;2)
- Shockley BJ, Croft DA, Anaya F (2007) Analysis of function in the absence of extant functional analogs: a case study of mesotheriid notoungulates. *Paleobiology* 33:227–247. <https://doi.org/10.1666/05052.1>
- Shockley BJ, Flynn JJ, Croft DA, Gans PB, Wyss AR (2012) New leonitiid Notoungulata (Mammalia) from Chile and Argentina: comparative anatomy, character analysis, and phylogenetic hypotheses. *Am Mus Novit* 3737:1–64. <https://doi.org/10.1206/3737.2>
- Silva M, Downing JA (1995) CRC Handbook of Mammalian Body Masses. CRC Press, New York
- Simpson GG (1945) A Deseado hegetothere from Patagonia. *Am J Sci* 243:550–564
- Simpson GG (1948) The beginning of the age of mammals in South America. Part I. *Bull Am Mus Nat Hist* 91:1–232

- Simpson GG (1967) The beginning of the age of mammals in South America. Part II. Bull Am Mus Nat Hist 137:1–260
- Simpson GG (1980) Splendid Isolation: The Curious History of South American Mammals. Yale University Press, New Haven, Connecticut
- Sinclair WJ (1908) The Santa Cruz Typothelia. Proc Am Philos Soc 47:64–78
- Sinclair WJ (1909) Mammalia of the Santa Cruz Beds. Volume VI, Paleontology. Part I, Typothelia. In: Scott WB (ed) Reports of the Princeton University Expeditions to Patagonia, 1896–1899. Princeton University, E. Schweizerbart'sche Verlagshandlung (E. Nägele), Stuttgart, pp 1–110
- Soria MF, Alvarenga HMF (1989) Nuevos restos de mamíferos de la Cuenca de Taubaté, estado de São Paulo, Brasil. An Acad Bras Cienc 61:157–175
- Sosa LM, García-López DA (2018) Structural variation of the masticator muscle in Typothelia (Mammalia, Notoungulata). Ser Correl Geol 34:53–70
- Solórzano A, Núñez-Flores M (2021) Evolutionary trends of body size and hypodonty in notoungulates and their probable drivers. Palaeogeogr Palaeoclimatol Palaeoecol 568:110306. <https://doi.org/10.1016/j.palaeo.2021.110306>
- Stirton RA (1953) A new genus of interatheres from the Miocene of Colombia. Univ Calif Publ Geol Sci 29:265–348
- Strömberg CAE, Dunn RE, Madden RH, Kohn MJ, Carlini AA (2013) Decoupling the spread of grasslands from the evolution of grazer-type herbivores in South America. Nat Commun 4:1478. <https://doi.org/10.1038/ncomms2508>
- Swartz SM (1989) The functional morphology of weight bearing: limb joint surface area allometry in anthropoid primates. J Zool 218:441–460 <https://doi.org/10.1111/j.1469-7998.1989.tb02556.x>
- Symonds MRE, Blomberg SP (2014) A primer on phylogenetic generalised least squares. In: Garamszegi LZ (ed) Modern Phylogenetic Comparative Methods and Their Application in Evolutionary Biology: Concepts and Practice. Springer Berlin Heidelberg, Berlin, Heidelberg, pp 105–130
- Tonni EP, Nabel P, Cione AL, Etchichury M, Túfalo R, Scillato-Yané G, San Cristóbal J, Carlini A, Vargas D (1999) The Ensenada and Buenos Aires formations (Pleistocene) in a quarry near La Plata, Argentina. J South Am Earth Sci 12:273–291
- Townsend KE, Croft DA (2008) Diets of notoungulates from the Santa Cruz Formation, Argentina: new evidence from enamel microwear. J Vertebr Paleontol 28:217–230
- Tsubamoto T (2014) Estimating body mass from the astragalus in mammals. Acta Palaeontol Pol 59:259–265
- Van Valkenburgh B (1990) Skeletal and dental predictors of body mass in carnivores. In: Damuth J, MacFadden BJ (eds) Body Size in Mammalian Paleobiology: Estimation and Biological Implications. Cambridge University Press, Cambridge, United Kingdom, pp 181–205
- Vera B (2012) Postcranial morphology of *Notopithecus* Ameghino, 1897 (Notoungulata, Interatheriidae) from the middle Eocene of Patagonia, Argentina. J Vertebr Paleontol 32:1135–1148. <https://doi.org/10.1080/02724634.2012.694320>
- Vera B (2016) Phylogenetic revision of the South American notopithecines (Mammalia: Notoungulata). J Syst Palaeontol 14:461–480. <https://doi.org/10.1080/14772019.2015.1066454>
- Vera B (2017) Patagonian Eocene Archaeopithecidae Ameghino, 1897 (Notoungulata): systematic revision, phylogeny, and biostratigraphy. J Paleontol 91:1272–1295. <https://doi.org/10.1017/jpa.2017.53>
- Villarroel C (1974a) Les mésothérinés (Notoungulata, Mammalia) du Pliocène de Bolivie. Leurs rapports avec ceux d'Argentine. Ann Paleontol 60:245–281
- Villarroel C (1974b) Un mésothériné nouveau (Notoungulata, Mammalia) dans le Miocène supérieur de Bolivie. C R Acad Sci Paris Sér D 279:551–554
- Villarroel C, Colwell Danis J (1997) A new leontiniid notoungulate. In: Kay RF, Madden RH, Cifelli RL, Flynn JJ (eds) Vertebrate Paleontology in the Neotropics: The Miocene Fauna of La Venta, Colombia. Smithsonian Institution Press, Washington, D.C., pp 303–318
- Vizcaíno SF, Cassini GH, Toledo N, Bargo MS (2012) On the evolution of large size in mammalian herbivores of Cenozoic faunas of southern South America. In: Patterson BD, Costa LP (eds) Bones, Clones, and Biomes. The History and Geography of Recent Neotropical Mammals. University of Chicago Press, Chicago, pp 76–101
- Welker F, Collins MJ, Thomas JA, Wadsley M, Brace S, Cappellini E, Turvey ST, Reguero M, Gelfo JN, Kramarz A, Burger J, Thomas-Oates J, Ashford DA, Ashton PD, Rowsell K, Porter DM, Kessler B, Fischer R, Baessmann C, Kaspar S, Olsen JV, Kiley P, Elliott JA, Kelstrup CD, Mullin V, Hoffreiter M, Willerslev E, Hulbin J-J, Orlando L, Barnes I, MacPhee RDE (2015) Ancient proteins resolve the evolutionary history of Darwin's South American ungulates. Nature 522:81–84. <https://doi.org/10.1038/nature14249>
- Wilson LAB, Sánchez-Villagra MR, Madden RH, Kay RF (2012) Testing a developmental model in the fossil record: molar proportions in South American ungulates. Paleobiology 38:308–321. <https://doi.org/10.1666/11001.1>
- Wickham H (2022) stringr: Simple, Consistent Wrappers for Common String Operations, R package version 1.4.1. R Foundation for Statistical Computing, Vienna, Austria. <https://CRAN.R-project.org/package=stringr>. Accessed October 9, 2022.
- Wickham H, Bryan J (2022) readxl: Read Excel Files, R package version 1.4.1. R Foundation for Statistical Computing, Vienna, Austria. <https://CRAN.R-project.org/package=readxl>. Accessed October 9, 2022.
- Wickham H, Seidel D (2022) scales: Scale Functions for Visualization, R package version 1.2.1. R Foundation for Statistical Computing, Vienna, Austria. <https://CRAN.R-project.org/package=scales>. Accessed October 9, 2022.
- Wickham H, Averick M, Bryan J, Chang W, McGowan L, François R, Grolemund G, Hayes A, Henry L, Hester J, Kuhn M, Pedersen T, Miller E, Bache S, Müller K, Ooms J, Robinson D, Seidel D, Spinu V, Takahashi K, Vaughan D, Wilke C, Woo K, Yutani H (2019) Welcome to the Tidyverse. J Open Source Softw 4. <https://doi.org/10.21105/joss.01686>
- Xie Y, Cheng J, Tan X (2022) DT: A Wrapper of the JavaScript Library 'DataTables', R package version 0.26. R Foundation for Statistical Computing, Vienna, Austria. <https://CRAN.R-project.org/package=DT>. Accessed October 21, 2022.
- Zhu H (2021) kableExtra: Construct Complex Table with 'kable' and Pipe Syntax, R package version 1.3.4. R Foundation for Statistical Computing, Vienna, Austria. <https://CRAN.R-project.org/package=kableExtra>. Accessed August 14, 2022
- Zihlman AL, Underwood CE (2013) Locomotor anatomy and behavior of patas monkeys (*Erythrocebus patas*) with comparison to vervet monkeys (*Cercopithecus aethiops*). Anat Res Int 2013:409534. <https://doi.org/10.1155/2013/409534>
- Springer Nature or its licensor (e.g. a society or other partner) holds exclusive rights to this article under a publishing agreement with the author(s) or other rightsholder(s); author self-archiving of the accepted manuscript version of this article is solely governed by the terms of such publishing agreement and applicable law.